Effect of additives in aqueous electrolytes on CO2 electroreduction

Samaneh Sharifi Golru^{1,2}, Elizabeth J. Biddinger^{1,2}*

¹ Department of Chemical Engineering, The City College of New York, CUNY, New York
(USA)

² Ph.D. Program in Chemistry, The Graduate Center of the City University of New York, New York (USA)

Abstract

Electrochemical reduction of CO₂ (CO2ER) is a promising technology to mitigate the CO₂ level in the atmosphere, as well as, to produce value-added chemicals and fuels. Aqueous solutions are regarded as the most common electrolytes for CO2ER. However, there are some challenges such as low CO₂ solubility and the presence of parasitic hydrogen evolution reaction which cause CO2ER in aqueous electrolytes to be inefficient in terms of selectivity and activity. A number of strategies have been proposed to enhance the efficiency for CO2ER in aqueous electrolytes. Among them, introducing additives to the aqueous solutions has attracted considerable attention. Depending on the chemical and physical properties of the additives, they have been demonstrated to improve the selectivity and activity in CO2ER. Herein, we provide a review on classification, mechanism, challenges, and perspectives of the additives in the aqueous electrolytes for CO2ER.

 $\label{eq:Keywords: CO2} \textbf{ Electroreduction, Aqueous electrolytes, Electrolyte effects,} \\ \textbf{ Electrocatalysis}$

1. Introduction

Carbon dioxide emissions are a key contributor to global warming and climate change. CO₂ electroreduction (CO2ER) is a promising method of utilizing some of the CO2 emissions to produce valuable chemicals and fuels^{1, 2}. However, CO2ER is not efficient enough due to the presence of the competing hydrogen evolution reaction (HER), the requirement for high overpotentials and poor product selectivity¹. The mechanism of CO2ER on metal electrodes is not yet fully determined. Most of the research in the field has focused on the development of the electrocatalysts and understanding the impact of catalyst morphology on the reaction ^{3,4}. However, there are not enough studies on the role of the electrolytes which are an essential component in CO2ER. Therefore, further research is required to elucidate the electrolyte effect. It has been reported that many electrolyte-related factors such as bulk and local pH⁵⁻²¹, electrolyte composition²²⁻³³, and electrolyte concentration^{17, 20, 21, 34-40} significantly influence the CO2ER. Using a small amount of additives in aqueous electrolytes has been reported as a promising method to enhance CO2ER^{28, 33, 40-60}. Depending on the species in the electrolytes, the interfacial structure, adsorption and stability behavior of intermediates can be influenced. In this article, we aim to overview recent studies conducted on the effect of additives in aqueous electrolytes on heterogeneous electrocatalytic CO₂ reduction. First, we discuss the aqueous electrolytes and their advantages and disadvantages. Second, the effect of cations and anions of the additives in aqueous electrolytes on CO2ER are explained. Then, the impact of additives on the interfacial structure will be also described. The techniques to study the electrode/electrolyte interface are examined. Finally, the existing challenges and future perspectives are presented.

2. Aqueous electrolytes and additives

The vast majority of the electrolytes used in CO2ER are based on aqueous solutions. Organic solvents²⁵⁻²⁷ and ionic liquids (ILs)²⁸⁻³⁰ have also shown promising results in CO2ER. Each electrolyte family has advantages and disadvantages (Fig. 1). CO₂ solubility in most organic solvents and ionic liquids is higher than that in aqueous electrolytes. For example, CO₂ solubility values in acetonitrile as an organic solvent and in 1-ethyl-3-methylimidazolium bis(trifluoromethylsulfonyl) imide ([Emim][NTF₂]) (also see list of abbreviations at end of article) IL are 0.279 and 0.130 M, respectively, while CO₂ solubility in aqueous electrolytes is 0.033 M at 25 °C and 1 atm⁶¹. However, some disadvantages such as toxicity, flammability, and low conductivity of organic solvents, or the high cost, high viscosity, low conductivity and incapability of ionic liquids to make hydrocarbons are limitations for using these solvents as electrolytes for practical CO2ER systems⁶².

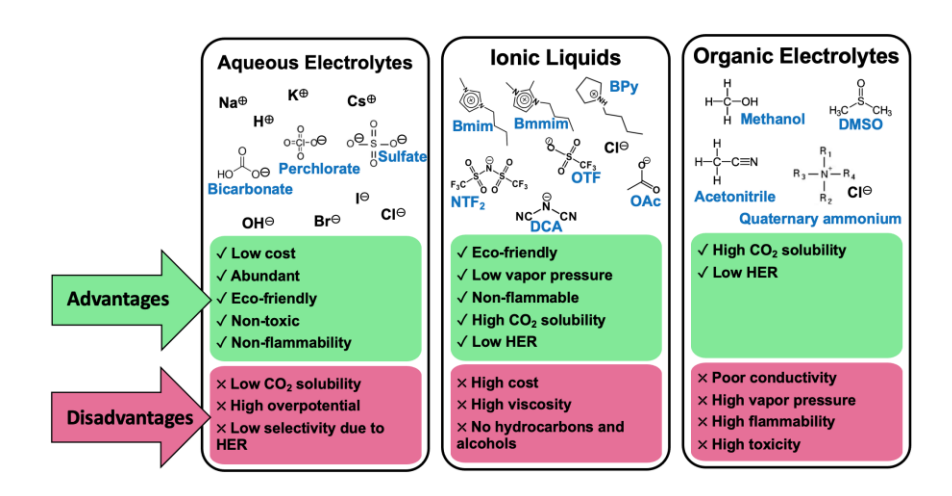


Fig. 1. Advantages and disadvantages of electrolyte families used for CO2ER.

CO₂ electroreduction in aqueous electrolytes is most popular due to advantages such as low cost, non-toxicity, eco-friendly nature, and material abundance ^{8, 33, 63, 64}. However, the CO₂

electroreduction efficiency in the aqueous electrolytes is not high enough due to the presence of the competing hydrogen evolution reaction (HER).

Bicarbonate-based aqueous electrolytes with a neutral pH are the most common solutions for CO₂ reduction. Besides the low cost and environmentally friendliness, they have an ability to buffer the local pH in the electrode/electrolyte interface^{10,65}.

In addition to bicarbonate, KOH-based electrolytes have also shown promising results since high pH favors ethylene formation and suppresses HER^{18, 22, 24, 48, 49}. Highly alkaline KOH solutions are problematic to be used in H-type electrochemical cells because KOH reacts with active CO₂ and produces inactive carbonate^{49, 65}. However, electrochemical flow cells with gas diffusion electrodes (GDE) have an ability to perform CO2ER in alkaline solutions. This ability is due to the separate flow paths of the catholyte and the inlet CO₂ gas which causes CO₂ molecules to be reduced to products as soon as they reach the catalyst-electrolyte interface⁶⁶. Moreover, since KOH does not have a buffering capability, the local pH will immediately increase in H-type cells, however, the stream of fresh electrolyte in flow cells will mitigate the pH rise ¹⁷. It needs to be mentioned that beside the advantages of the flow cells such as high current density, there are some issues with flow cells which need to be addressed/taken into consideration in the FE or partial current density calculations. Salt deposition on GDE⁴⁹, electrode flooding^{67, 68}, crossover of CO₂ to the anode⁶⁹, and also migration of liquid products⁷⁰ through the membrane and GDE are important challenges in using flow cells.

Using additives can be a promising strategy to enhance CO2ER in aqueous electrolytes since the advantages of both additive and aqueous electrolytes can be simultaneously achieved ^{28, 33, 40-60} (Fig. 2). Additives can impact CO2ER by influencing the CO₂ concentration at the surface, local pH, intermediate adsorption, local electric field, viscosity and conductivity ^{50, 53, 54, 60, 71, 72}. From

the conductivity perspective, it needs to be mentioned that ohmic loss is significant in the electrolytes with low conductivity. Therefore, iR compensation should be carried out before data analysis to compensate for the solution resistance in these electrolytes. The quantity and type of the additives should be carefully chosen according to the catalyst material, the supporting electrolyte, and the reaction of interest. Not all of additives are able to improve CO2ER. For example, additives such as dicyanamide ([DCA]⁻)-based salts which may strongly coordinate with the surface, compete with adsorbed CO, the key intermediate in CO2ER, and consequently, suppress further reduction of CO to hydrocarbons and alcohols⁴¹. In the next section, we will discuss different types of additives that have been used in the aqueous electrolytes, and also the effect of anions and cations of ionic additives on CO2ER.

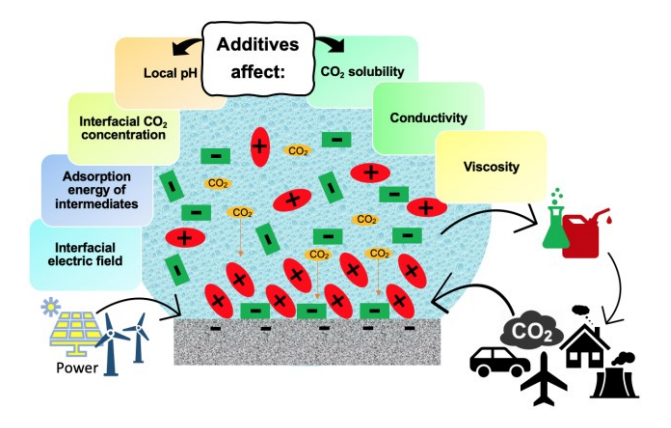


Fig. 2. The impact of additives in the aqueous electrolytes on CO2ER.

3. Ionic species

Ionic additives including organic salts⁵⁰, surfactants^{51, 73}, and ionic liquids^{41, 50, 53, 54, 60} have been used to enhance the CO2ER in aqueous electrolytes (Table 1). The nature, specific adsorption, hydrophobicity and size of the ionic species play a crucial role in CO2ER in aqueous

electrolytes ^{2, 20, 21, 24, 36, 39, 41, 49, 52-54, 59, 71, 72, 74-92}. The intrinsic properties of both anions and cations are important in CO2ER and they can alter the reactions through competing or synergistic effects.

Ionic additives can affect CO2ER in different ways. Some salts have an ability to change the catalyst morphology during CO2ER. For example, Thevenon et al. reported that adding an organic salt, N,N'-ethylene-phenanthrolinium dibromide can generate a nanostructured morphology on Cu during CO2ER in an aqueous electrolyte which can produce C₂₊ products with 70% FE for more than 40 hr. ⁵⁰. During electroreduction, an organic film was deposited on the surface which was likely the reason for inhibiting HER and the high stability of the nanostructure morphology of the catalyst ⁵⁰.

Some additives have been also reported to enhance CO2ER by accumulating at the surface and suppressing HER. Banerjee et. al showed that adding cationic surfactant, cetyltrimethylammonium bromide (CTAB), to 0.1 M NaHCO3 electrolyte could enhance the formate faradaic efficiency (FE) from 5% to 50% on a Cu catalyst at -0.6 V vs RHE⁵¹. CTAB could significantly suppress HER by blocking the accessibility of the protons to the surface⁵¹. Electrochemical impedance spectroscopy (EIS) results showed that CTAB decreased the double layer capacitance which can be indicative of displacement of H₃O⁺ and Na⁺ ions by CTAB molecules at the interface. Also, they reported that increasing the concentration and the alkyl chain length of the surfactant can further enhance CO2ER⁵¹.

There are other types of additives such as ILs which can enhance CO2ER by promoting CO₂ adsorption, make a complex with intermediates and reduce the activation energy (overpotential) to produce CO2ER products ^{28, 60, 93} (Fig. 3). Rosen et al. obtained 96% FE for CO on Ag catalysts by using a concentrated IL/water mixture (18 mol% (70 wt.%) 1-ethyl-3-methylimidazolium

tetrafluoroborate ([Emim][BF4]) in water) ²⁸. They also showed that [Emim][BF4] can reduce the CO2ER overpotential to less than 0.2 V, likely due to complexation of intermediates-IL²⁸.

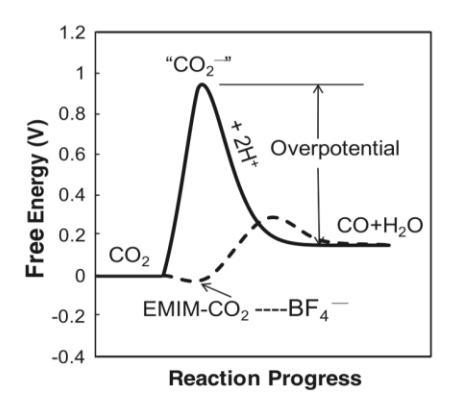


Fig. 3. A schematic of how ILs can reduce the energy barrier for CO2ER. Reprinted from Rosen et al. Copyright (2011), with permission from AAAS²⁸.

The concentration of the additives also plays a key role in CO2ER. Neubauer et al. studied the effect of the concentration of 1-ethyl-3-methylimidazolium trifluoromethanesulfonate ([EMIM][OTF]) (0-50 mol %) in 10 mM KHCO3 on CO2ER on Ag⁶⁰. They reported that no CO2 reduction was observed for IL concentrations below 2.5 mol%⁶⁰. A significant CO2 reduction was obtained for the electrolytes with more than 20% IL⁶⁰. The CO formation was enhanced by increasing the IL concentration to 50% where 95.6% FE for CO was observed⁶⁰. They attributed this observation to blocking H₂O diffusion to the surface at high IL concentrations⁶⁰.

So far, we have discussed on how ionic additives contribute to enhance CO2ER. As mentioned earlier, CO2ER is highly influenced by the physical and chemical properties of the additive ions even in diluted electrolytes with a high water content. A number of studies have been conducted on the effect of anions^{21, 37-39, 49, 52-54, 59, 74, 78-81, 83-85, 92} and cations ^{24, 36-38, 71, 72, 86-90, 94} of the ionic

additives. In the next sections, we will focus on how changing anions and cations affects the CO2ER.

Table 1. Selected examples of ionic additive-containing aqueous electrolytes used for CO₂ reduction on different metals.

Additive	Main electrolyte	Catalyst	Potential	Current density (mA/cm²)	FE (%) for main products	Ref.
Blank 10 mM N,N'- ethylene- phenanthrolinium dibromide	0.1 M KHCO ₃ / H ₂ O	Cu	-1.07 V vs. RHE	3.8	26.0% C ₂ 63.6% C ₂	50
Blank 67 μM CTAB	0.1 M KHCO ₃ / H ₂ O	Cu	-0.6 V vs. RHE	~0.1° (j _{HCOO-}) ^b ~0.7 (j _{HCOO-})	~5% HCOO ⁻	51
Blank 10 mM tolyl-pyr chloride	0.1 M KHCO ₃ / H ₂ O	Cu	-1.1 V vs. RHE	4.46	26.0% C ₂₊ 78.2% C ₂₊	47
18 mol% [Emim][BF ₄]	H ₂ O	Ag	1.5 V (cell voltage)	N.R.°	96 % CO	28
50 mol% [Emim][OTF]	10 mM KHCO ₃ / H ₂ O	Ag	-1.8 vs. Ag/AgCl	~6.1	95.6 ± 6.8% CO	60
30 wt.% [Bmim][Cl] 40 wt.% [Bmim][Cl] 60 wt.% [Bmim][Cl] 60 wt.% [Bmim][Cl]	H ₂ O	Ag	-1.5 V vs. SCE	N.R.	50% CO 70% CO 99% CO >99% CO	40
0.5 M [Emim][DCA]	H ₂ O	Sn powder	-1.2 V vs. RHE	~ 0.633	81.9% HCOO-	57
Blank 40 mM [Bmim][BF ₄]	0.1 M KHCO ₃ / H ₂ O	Cu nanoporous foam	-1.6 V vs. Ag/AgCl	~10 ~20	N.R. 49% C ₂ H ₅ OH	44
4 mol% [Emim][BF ₄]	H ₂ O	MoS ₂	-0.761 V vs. RHE	42	~100% CO	88

3.1. Anion effect

^a Values with ~ were derived from the graphical results.

^b j: Partial current density for a specific product, not total current density.

^c N.R.: Not reported in the article.

The adsorption of the anions on the electrode surface due to electronic and chemical forces can significantly impact the mechanism and kinetics of CO₂ electroreduction (Table 2)^{38, 74}. However, the mechanism of the anion adsorption on the negatively charged electrode during CO2ER is not fully understood. The adsorption of anions can impact the electrochemical reactions in several ways: i) adjusting the local pH⁷⁴, ii) altering the catalyst morphology^{50, 53, 80, 95-97}, iii) affecting the surface adsorption energy and binding strength of the intermediates to the electrode surface^{96, 98}, and iv) blocking the active sites needed for the adsorption of the intermediates and reactants⁹⁶.

Anions can influence CO2ER by changing the local pH at the interface. Local pH is an important parameter in the product selectivity because the rate determining step for some reactions in CO2ER is pH-dependent^{99, 100}. Some anions such as bicarbonate and phosphate are able to buffer the local pH which increases due to the generation of OH⁻ as a product of CO2ER and HER. Hori et al. showed that product selectivity on Cu was significantly impacted by the anion nature⁷⁴. Cl⁻, ClO₄⁻, dilute HCO₃⁻ (0.1 M), and SO₄⁻ favored ethylene and alcohols formation on Cu, while concentrated HCO₃⁻ (0.5 M) and H₂PO₄⁻ produced more methane⁷⁴. Concentrated HCO₃⁻ and H₂PO₄ -based electrolytes had an ability to buffer the pH rise due to reduction reactions⁷⁴. However, the local pH in Cl⁻, ClO₄⁻, dilute HCO₃⁻, and SO₄⁻ -based electrolytes became more alkaline due to lack of the buffering ability and consequently, enhanced ethylene formation⁷⁴. The higher formation of ethylene in alkaline media can be justified by the mechanism proposed for methane and ethylene formation on Cu catalysts⁹⁹(Fig. 4). As can be seen in Fig. 4, there are two pathways for formation of hydrocarbons on Cu⁹⁹. Methane is produced through the first pathway in which the rate determining step (RDS), CO protonation, is directly proportional to the proton concentration. Ethylene can be produced through two pathways⁹⁹. In addition to the first pHdependent pathway which needs a high overpotential to produce ethylene, there is also another

pathway proposed for ethylene formation in which the CO dimerization, as the RDS, is pH-independent (no proton involved)⁹⁹. Therefore, it is expected that the selectivity toward ethylene is enhanced in alkaline media due to suppressing methane and hydrogen formation ⁹⁹.

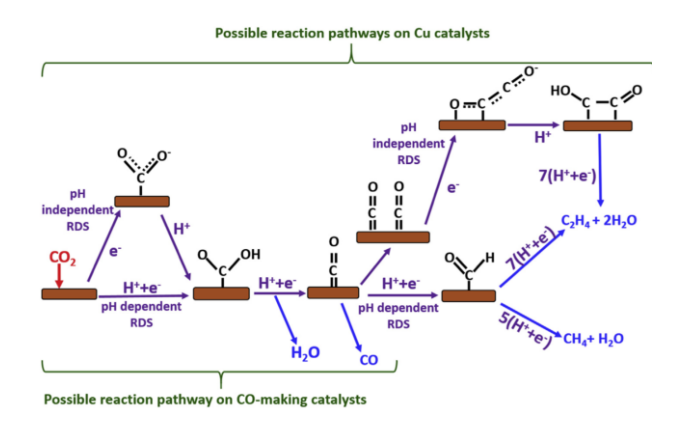


Fig. 4. CO₂ electroreduction mechanism for different products. Reprinted from Varela, Copyright (2020), with permission from Elsevier⁹⁹.

The ability of the anions to specifically adsorb on the surface is also an important factor in CO2ER. The specific adsorption of anions is inversely correlated to the solvation energy of the ions¹⁰¹. The specific adsorption of a series of anions on the metal surfaces has been reported to increase in the following order F⁻ < CIO₄⁻ < SO₄² - < CI⁻ < Br⁻ < I⁻¹⁰¹. In a theoretical study using DFT, McCrum et al. also showed that CI⁻, Br⁻, and I⁻ have a strong ability to adsorb on the Cu surface, especially on Cu (100)¹⁰², the main facet for C₂ product formation in CO2ER¹⁰³. Adsorption of the anions on the electrode has been reported to positively ⁵²⁻⁵⁴, ⁸⁵, ⁹⁵, ¹⁰⁴⁻¹⁰⁶ or negatively ²², ¹⁰⁷ influence CO2ER. Researchers have shown that the presence of CI⁻ anions adsorbed on Ag electrodes can significantly enhance CO2ER⁹⁵. They showed that the enhanced activity in CO2ER is not only due to the morphology change created in the presence of CI⁻, since a similar nanostructured Ag but without CI⁻ anions didn't show the same activity⁹⁵. They believe

that the thin layer of Cl⁻ anions adsorbed to the surface is the reason for suppressing HER and enhancing CO2ER⁹⁵. In another study, Gao et al. investigated the role of halide anions (Cl⁻, Br⁻, and I⁻) in CO2ER in a buffer-based electrolyte (0.1 M KHCO₃) on an oxidized polycrystalline Cu electrode⁵³. A change in morphology of the Cu electrode was observed for all halides especially for I⁻ containing electrolytes⁵³. Although the FE was not significantly altered in the presence of halides, the total current density and formation rate for C2 products were enhanced in the order of $Cl^- \le Br^- \le I^{-53}$. The results showed that the activity and formation rate of C_2 products are linearly proportional to the anion adsorption energy⁵³. Nanostructuring and the subsurface oxygen also promoted the anion adsorption on the surface⁵³. Gao et al. believe that using buffer electrolytes rules out the possibility that local pH change is the reason for different activity observed for the halides⁵³. They attributed the superior performance of the system mainly to the adsorption of halide ions on oxidized-Cu, although change in the morphology and subsurface oxygen could also contribute to the enhanced activity of the catalyst⁵³. The presence of the anions adsorbed on the surface can enhance CO₂ adsorption and in turn, formation and stabilization of *COOH intermediates by partial charge donation from the halide ions to stable CO₂ molecules⁵³.

Anions can also impact the CO coverage, as the main intermediate in CO2ER, on the surface. Huang et al. showed that adsorption of anions enhanced the CO* adsorption⁵². They studied the effect of anions (ClO₄⁻, Cl̄-, Br̄-, Ī-) with same cation (K⁺) on CO2ER over Cu (100) and Cu(111)⁵². They observed that C₂ products formation was enhanced in the order of ClO₄⁻<Cl̄-<Br̄-< Ī-. A 74% increase for C₂-C₃ products was observed for KI. The surface roughness also increased after electrolysis⁵². Although, change in local pH and morphology may contribute to the selectivity, the researchers believe that the superior performance observed in the KI electrolyte was attributed to the high CO* coverage on the electrode⁵². In another study, Shaw

et al. also showed adsorption of F⁻ and Cl⁻ anions on the surface can increase the binding energy of CO* on Cu electrodes ¹⁰⁴. Adsorption of anions can also alter the electronic structure of Cu so that more positive charge on CO* molecules is induced ¹⁰⁵.

CO₂ molecules have a low affinity to the Cu surface¹⁰⁸. Anions have an ability to promote the CO₂ adsorption on the electrode surface. Ogura et al. reported an enhancement in ethylene formation in CO2ER on Cu in the presence of halide anions (Cl $^-$, Br $^-$, I $^-$) with K $^+$ cations 85 . Halides strongly adsorb on the surface and block the hydrogen adsorption. However, they can enhance CO₂ adsorption to the surface and stabilize the intermediates due to the charge transfer from anions to CO₂ vacant orbital^{85, 106} (Fig. 5a). These results are in agreement with Huang's⁵² and Shaw's 104 studies (mentioned earlier) in which anion adsorption on the surface favored CO2ER. Fig. 5a shows the schematic of the double layer in the presence of KBr in the electrolyte. It has been reported that specifically adsorbed halides and solvated cations are located at the inner Helmholtz plane (IHP) and outer Helmholtz plane (OHP), respectively 109. Electron transfer from halide to CO₂ brings CO₂ molecules to the IHP. *COOH is then formed via interaction of CO₂ with a proton and directly adsorbs to the metal surface. Solvated cations also have some interactions with oxygen of CO₂ molecules. The interaction between cations, CO₂ and adsorbed halides can reduce the activation energy for CO₂ reduction by weakening the C-O bond. Strong adsorption of anions positively impacts CO₂ reduction onset potential⁸⁵.

In another report, Varela et al. demonstrated that FE can be also influenced by adding halides to a buffer electrolyte in CO2ER on Cu⁵⁴. Results showed that FE_{CO} was enhanced from \sim 7 to \sim 14% and \sim 27% at -0.95 V vs. RHE by adding 0.3 M KBr and KCl, respectively, to the buffer electrolyte. However, KI-added electrolytes showed an enhancement in methane selectivity (\sim 37% FE_{CH4} at -0.95 V vs. RHE)⁵⁴ (Fig. 5b-c). They believe that halides can enhance the negative charge

on the surface in the order of $Cl^- < Br^- < I^{-54}$. Methane formation in KI can be attributed to the more facilitated protonation of CO due to the large amount of negative charge from adsorption of I^- anions (Fig. 5d)⁵⁴.

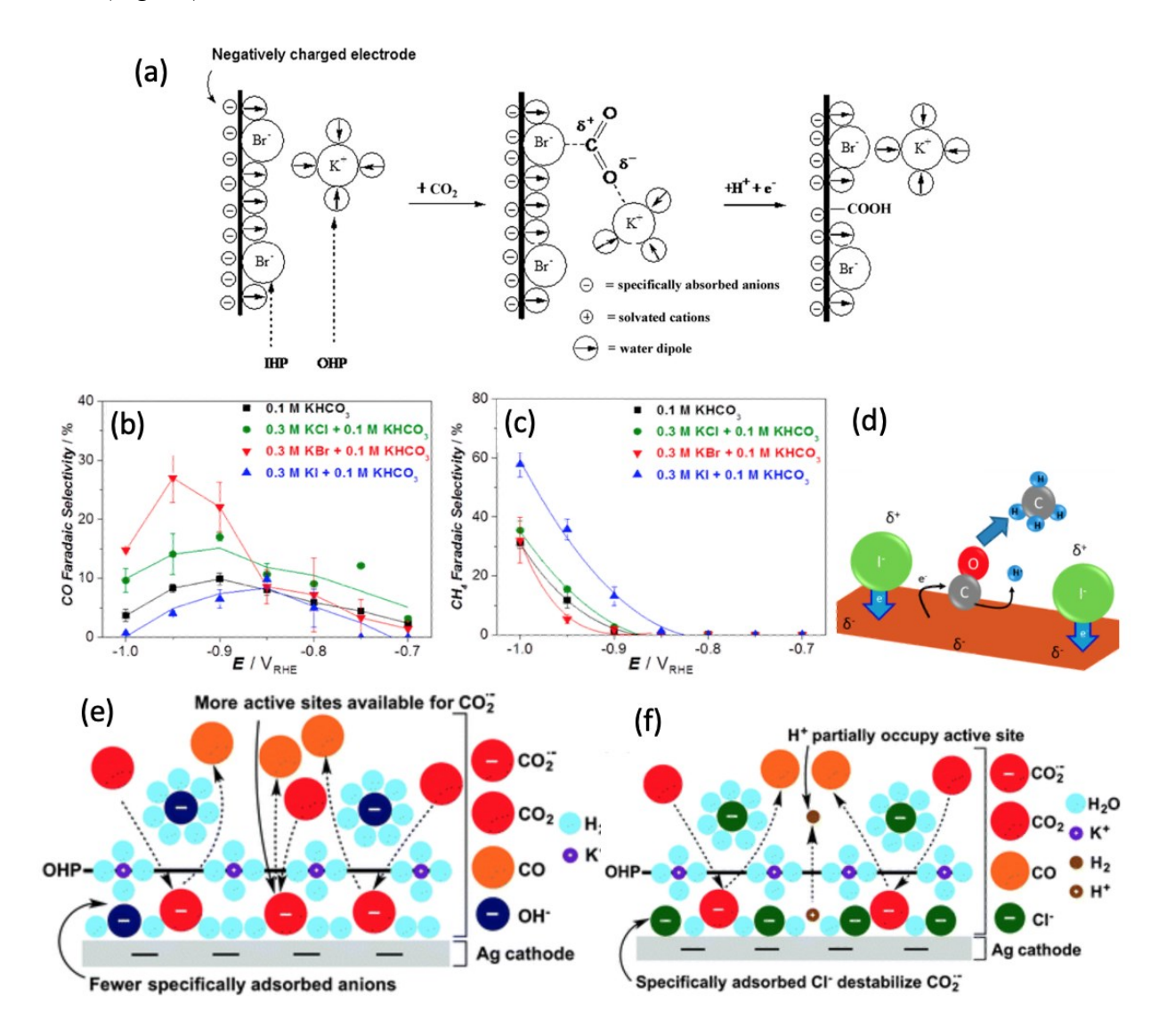


Fig.5. Anion effect on the surface in CO2ER; a) A schematic of the double layer, adsorbed Br⁻ anions, CO₂ and K⁺ cations during CO2ER; Faradic efficiencies of CO (b) and CH₄ (c) in 0.1 M KHCO₃ and 0.3 M KCl, KBr, KI. d) protonation of CO in the presence of I⁻ on the surface; A schematic of the double layer in the presence of e) KOH and f) KCl during CO2ER over Ag

electrodes. Figure 5a is reprinted from Ogura et al. Copyright (2010), with permission from Elsevier⁸⁵. Figure 5b, 5c, and 5d are reprinted with permission from Varela et al. Copyright (2016) American Chemical Society⁵⁴. Figure 5e and 5f are Reproduced from Verma et al. Copyright (2016), with permission from The Royal Society of Chemistry²².

In opposite to the studies which reported anion adsorption can enhance CO2ER52-54, 85, 104, 106 (discussed above), there are other studies which indicate that the adsorption of anions on the surface have a negative impact on CO2ER^{22, 41, 107}. For example, Verma et. al. studied the effect of adding a series of anions with K⁺ cation on CO2ER²². They showed that large anions (such as Cl⁻) can directly adsorb on the Ag surface and suppress CO2ER by destabilizing the intermediates (Fig. 5e-f)²². However, small anions (like OH⁻) which have a larger solvation shell electrostatically interact with the surface ²². They also found the onset potential and charge transfer resistance in CO2ER on Ag in the order KOH < KHCO₃ < KCl ²². They attributed this effect to the interaction of anions with intermediates and stabilizing them on the surface²².

Kortlever et al. also studied the effect of potassium-based salts with different anions (0.1 M KCl, KBr, KI, KClO₄ and K₂SO₄) in a phosphate buffer (0.1 M K₂HPO₄ + 0.1 M K₃PO₄) on CO2ER over Cu catalysts¹⁰⁷. The results showed that by adding KBr and KI to the electrolyte, the peak attributed to the CO₂ reduction in CVs disappeared¹⁰⁷. Also, KBr and KI showed a higher current density in CVs compared to other salts¹⁰⁷. The authors attributed these observations to the ability of Br⁻ and I⁻ ions to strongly adsorb on the surface¹⁰⁷. The strong adsorption of anions can enhance HER and suppress the CO2ER¹⁰⁷. These results contradict with what have been reported earlier in this section ^{52-54, 85, 95, 104-106}.

Beside the effect of anions in the inorganic salt additives, anions in ILs can also play a key role in the interfacial structure^{29, 41, 110}. Recently, we investigated the effect of adding 10 mM of a series of imidazolium ILs with the same cation 1-butyl-3-methylimidazolium ([Bmim]⁺) and different anions (bis(trifluoromethylsulfonyl)imide ([NTF₂]⁻), triflate ([OTF]⁻), dicyanamide ([DCA]⁻), acetate ([Ac]-), and chloride Cl-) in CO2ER on Cu catalyst⁴¹. We found by adding ILs to a buffer solution (0.1 M KHCO₃), the FE for formate increased compared to the IL-free electrolyte⁴¹. The maximum increase in FE_{formate} was observed for [Bmim][NTF₂] (38.7% FE). This can be due to the high hydrophobicity and high CO₂ absorption capacity of [Bmin][NTf₂] ⁴¹. Also, we found a very low FE for hydrocarbons (~7% at -1.12 V vs. RHE) and a very high FE for hydrogen (~75% at -1.12 V vs. RHE) for [Bmim][DCA] 41. By using XPS, we showed that [Bmim][DCA] can strongly adsorb to the surface and this adsorption can be the reason for having a high selectivity toward hydrogen⁴¹. The strongly adsorbed [DCA]⁻ anions can poison the surface. Since [DCA]⁻ anions have a high hydrophilicity, they can adsorb water molecules and enhance HER⁴¹. Due to low CO₂ absorption capacity of ILs with [DCA] anions, [DCA] can repel CO₂ molecules from the surface and suppress CO2ER⁴¹.

It should be mentioned that the specific adsorption of anions is not the only factor determining the selectivity and activity in CO2ER. The intrinsic properties of the anions are also crucial. It has been reported that Cl⁻ anions can enhance CO2ER to CO formation on Au due to the high strong specific adsorption ability of Cl⁻. However, HPO4²⁻ anions which also had a higher specific adsorption strength compared to SO4²⁻ and HCO3⁻ had a lowest FE_{CO}. This observation was attributed to the strong buffer ability of HPO4²⁻ anions which creates a lower local pH and enhances HER⁵⁹. In the next section, we will review the effect of cations in the electrolytes in CO2ER.

Table 2. Selected examples of CO₂ reduction in aqueous electrolytes containing additives with different anions.

Additive	Main electrolyt e	Catalyst	Example potential	Current density (mA/cm²)	FE (%) for main products	Ref.	
1 M KHCO ₃	H ₂ O	Nanoporous	-0.67 V RHE	~60a	~5% C ₂₊		
1 M KOH		Cu		~653	~62% C ₂₊	49	
0.5 M K ₂ SO ₄				~60	~14% C ₂₊		
1 M KCl				~150	~35% C ₂₊		
0.1 M KClO ₄	H ₂ O	Cu (100)	-1.23 V vs. RHE	~1.0	~30% C ₂ H ₄ , ~7% C ₂ H ₅ OH	52	
0.1 M KCl				~1.5	~40% C ₂ H ₄ , ~8% C ₂ H ₅ OH		
0.1 M KBr				~2.0	~45% C ₂ H ₄ , ~10% C ₂ H ₅ OH		
0.1 M KI				~7.0	~50% C ₂ H ₄ , ~16% C ₂ H ₅ OH		
Blank	0.1 M	Plasma-	-1.0 V vs. RHE	~29	58.9% C ₂ -C ₃	53	
0.3 M KCl	KHCO ₃ /	activated		~44	61.5% C ₂ -C ₃		
0.3 M KBr	H ₂ O	Cu		~52	58.4 % C ₂ -C ₃		
0.3 M KI				~55	61.7% C ₂ -C ₃		
Blank	0.1 M KHCO ₃ / H ₂ O	Cu	-0.95 V vs. RHE	~2.5	~8% CO, ~12% CH ₄	54	
0.3 M KCl		H ₂ O			~2.3	~14% CO, ~15% CH ₄	
0.3 M KBr				~0.7	~27% CO, ~4% CH ₄		
0.3 M KI				~6.0	~ 4% CO, ~37% CH ₄		
Blank	0.1 M KHCO ₃ /	Cu	-1.0 V vs. RHE	~5.5	9.4% C ₂ H ₄ , 2.0% C ₂ H ₅ OH	80	
4 mM KI	H ₂ O			~ 5	13.2% C ₂ H ₄ , 5.0% C ₂ H ₅ OH		
4 mM KCl				~ 10	15.0% C ₂ H ₄ , 7.7% C ₂ H ₅ OH		
4 mM KBr				~ 7.5	14.3% C ₂ H ₄ , 7.3% C ₂ H ₅ OH		
4 mM KF				~ 6.5	16.3% C ₂ H ₄ , 7.9% C ₂ H ₅ OH		
0.1-3 M KBr	H ₂ O	Cu-mesh	-1.80 V vs.	12.6	63% C ₂ H ₄	39	
0.1-3 M KI			Ag/AgCl	12	68.1% C ₂ H ₄		
0.1 M KHCO ₃	H ₂ O	Cu	-1.41 V vs. NHE	5	29.4% CH ₄ , 30.1% C ₂ H ₄	74	
0.1 M KCl			-1.44 V vs. NHE		11.5% CH ₄ , 47.8% C ₂ H ₄		

			,		1	
0.1 M KClO ₄			-1.40 V vs. NHE		10.2% CH ₄ , 48.1% C ₂ H ₄	
0.1 M K ₂ SO ₄			-1.40 V vs. NHE		12.3% CH ₄ , 46.0% C ₂ H ₄	
0.1 M K ₂ HPO ₄			-1.23 V vs. NHE		17.0% CH ₄ , 1.8% C ₂ H ₄	
0.5 M KCl			-1.39 V vs. NHE		14.5% CH ₄ , 38.2% C ₂ H ₄	
0.5 M K ₂ HPO ₄			-1.17 V vs. NHE		6.6% CH ₄ , 1.0% C ₂ H ₄	
0.1 M KHCO ₃	H ₂ O	Cu	-1.0 V vs. RHE	~0.9 (j _{CH4}) ^b , ~1.1 (j _{H2})	N.R.°	21
0.1 M KClO ₄				~0.15 (j _{CH4}), ~0.22 (j _{H2})		
0.1 M KSO ₄				~0.15 (j _{CH4}), ~0.23 (j _{H2})		
0.1 M KH ₂ PO ₄				~2.5 (j _{CH4}), ~2.1 (j _{H2})		
0.25 M KHCO ₃	0.25 M	Au	-0.7 V vs. RHE	~5.0	~70% CO	59
0.25 M KCl	KHCO ₃ / H ₂ O			~4.8	~82% CO	
0.25 M K ₂ HPO ₄ 0.25 M K ₂ SO ₄				~7.0	~10% CO ~69% CO	
Blank	0.1 M	Cu	-0.92 V vs. RHE	0.22 (j _{HCOO-})	9.01% HCOO-	41
10 mM [Bmim][NTF ₂]	KHCO ₃ /			1.43 (j _{HCOO-})	38.7% HCOO	
10 mM [Bmim][OTF]	H ₂ O			1.25 (јнсоо-)	19.5% HCOO ⁻	
10 mM [Bmim][Ac]				0.63 (j _{HCOO-})	18.3% HCOO ⁻	
10 mM [Bmim][Cl]				1.10 (j _{HCOO-})	22.7% HCOO-	
10 mM [Bmim][DCA]				0.56 (јнсоо-)	5.9% HCOO ⁻	

^a Values with ~ have not mentioned in the original article but derived from the graphical results.

3.2. Cation effect

Cations are another essential part in the electrolytes which significantly affect CO₂ electroeduction (Table 3) ^{24, 36, 38, 111-113}. Since CO2ER occurs at a much more negative potentials than potential of zero charge (PZC), adsorption of the hydrated cations to the metal surface is expected during electrolysis^{36, 114}. Opposite to the anions which can specifically adsorb on the surface, alkali cations do not directly adsorb on the surface, rather, they are located in the OHP^{87, 109, 115}. When halides strongly adsorb to the surface and attract CO₂ molecules, cations transfer to

^b j: Partial current density for a specific product, not total current density.

^c N.R.: Not reported in the article.

the OHP to compensate the charge (Figure 6)⁹². Adsorption of cations on the surface impacts CO2ER in different ways. Adsorbed cations can affect the intermediate stabilization^{72, 87, 92}, local pH^{86, 89, 91}, interfacial CO₂ concentration^{36, 86, 89, 91, 116}, interfacial electric field ^{34, 71, 86, 89, 117, 118}, and the interaction of the reactants on the surface ⁹⁰.

Size of the cations is a key parameter to influence the interfacial properties. Adsorption of the cations to the electrode surface is dependent on the degree of the cation solvation which is determined by the ion size ^{36, 119}. Small cations like Li⁺ do not directly adsorb on the surface due to their large hydration shell; however, large cations such as Cs⁺ and K⁺ will adsorb to the surface ¹²⁰. The lower degree of hydration for larger cations causes water molecules to be more detachable ⁹². Therefore, CO₂ molecules can directly interact with cations. This can facilitate the electron transfer from the electrode and stabilize the CO₂ (Fig. 6) ⁹².

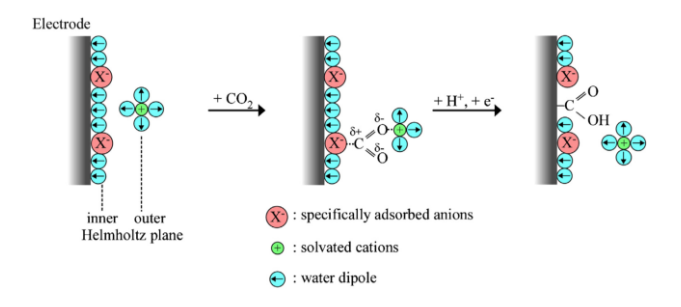


Fig 6. A schematic of the attraction of CO₂ molecules and formation of *COOH intermediates.

Reprinted from Ogura et al. Copyright (2013), with permission from Elsevier⁹².

Resasco et al. investigated the effect of cation size on the activity for different products over Ag, Sn, Cu (100), and Cu (111) ⁸⁷. Results showed that the cation size had a negligible effect on the H₂ partial current density for all metals⁸⁷. However, compared to small cations, larger cations had a higher activity for C₂ and formate products on Cu, and formate and CO for both Sn and Ag

electrodes⁸⁷. For example, by changing the cation from Li⁺ to Cs⁺, a 1100% increase in j_{ethylene}, 455% in j_{CO}, and 94% in j_{HCOO}- at -1.0 V vs. RHE was observed on Cu(100), Sn, and Ag, respectively⁸⁷. Using DFT calculations, they attributed this observation to the stabilized intermediates due to the interactions of hydrated cations in OHP and adsorbed species with large dipole moments such as *CO₂, *CO and *CO₂⁸⁷.

In one of the earliest studies on the effect of alkali cation size, Murata et al. investigated the effect of cation size on the product selectivity on Cu³⁶. They showed that the product selectivity toward ethylene was improved by 486%, with a constant 5 mA/cm² current density, when changing the cation from Li⁺ to Cs⁺ in a bicarbonate electrolyte³⁶. They attributed the variation in product selectivity to the local pH which is altered due to the specific adsorption of ions at the surface and the potential in OHP³⁶. The strongly solvated cations such as Li⁺, could not directly adsorb to the surface due to their large hydration shell. The potential of OHP for small cations is less positive than large ones. More negative OHP potentials for small cations attract protons to the surface and decrease the pH³⁶. For the same reason, large cations will create a higher pH at the interface³⁶. The higher potential in the OHP for large cations does not affect the uncharged CO₂, but it affects the proton transfer and increases the local pH. High local pH favors ethylene formation and suppresses HER³⁶.

In a computational study conducted by Singh et al., it was reported that pKa of the cation hydrolysis can be reduced at the interface due to the polarization of water molecules between positive cations and negative electrodes⁸⁶. Size of cations and the surface potential influence the pKa ⁸⁶. Since pKa for larger cations is lower than that for smaller ones, larger cations can act as buffers and prevent the pH rise. Lower pH at the interface will favor CO₂ adsorption to the surface and enhance the local CO₂ concentration ⁸⁶. The experimental results showed an enhancement for

C₂ products (42.5% FE_{C2} products at -1.0 V vs. RHE) and CO formation (80.3% FE_{C0} at -1.0 V vs. RHE) on Cu and Ag, respectively (Fig. 7a-c) ⁸⁶.

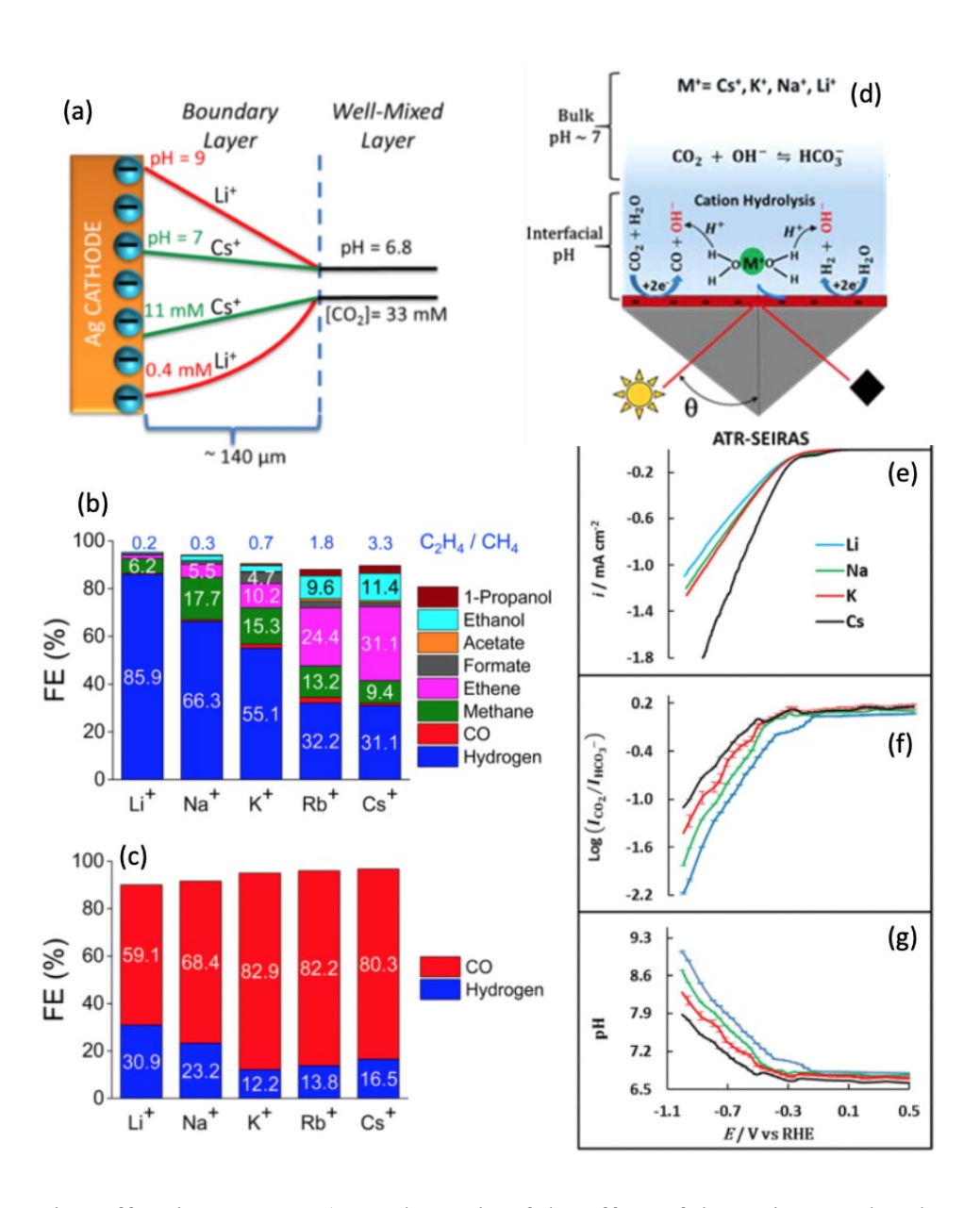


Fig. 7. Cation effect in CO2ER; a) A schematic of the effect of the cations on local pH; b and c) experimental results for FEs for Cu and Ag electrodes, respectively, in electrolytes containing different alkali cations; d) A schematic of how cation hydrolysis buffers the local pH; e) Total current density; f) intensity ratio of I co2/ I HCO3-; g) local pH as a function of potential in

aqueous electrolytes with different cations. Figure 7a-c are reprinted with permission from Singh et al. Copyright (2016) American Chemical Society⁸⁶. Figure 7d-g are reprinted with permission from Ayemoba et al. Copyright (2017) American Chemical Society¹¹⁶.

There are also several experimental studies conducted to investigate the relationship between local pH and CO2ER ^{89, 91, 116, 121}. Ayemoba et al. analyzed the interfacial pH in the electrolytes containing different size of alkali- cations on gold electrodes during CO2ER by ATR-SEIRAS¹¹⁶ (Fig. 7d). They found the local pH is proportional to the HCO3⁻/CO2 concentration ratio (Fig. 7f-g) ¹¹⁶. Their results were consistent with Singh's research findings that local pH decreases for larger cations⁸⁶.

In contrast to the studies mentioned above, several groups ^{89, 91} using in situ attenuated total reflectance-surface enhanced infrared absorption spectroscopy (ATR-SEIRAS) have shown that the local pH is not the reason for the superior performance of the large cations in CO and CO₂ reduction. Gunathunge et al. studied the effect of potential on the CO coverage as a key intermediate in CO reduction on Cu catalysts in the electrolytes with different cations (0.1 M LiDCO₃, KDCO₃, CsDCO₃)⁸⁹. They showed that the cation size significantly impacts the CO coverage on the surface⁸⁹. Based on the frequency shift observed for C≡O band, they reported an enhanced electric field for large cations⁸⁹(Fig. 8a). A sharp decrease in CO concentration was also observed for large cations (K⁺ and Cs⁺) by going to more negative potential which is due to faster kinetics for CO reduction in the presence of large cations (Fig. 8b) ⁸⁹. They believe that the drop in the CO coverage is mainly due to the strong interfacial electric field in the presence of large cations rather than change in the local pH⁸⁹. They also attributed the hysteresis observed in CVs to surface reconstruction due to the ion adsorption⁸⁹.

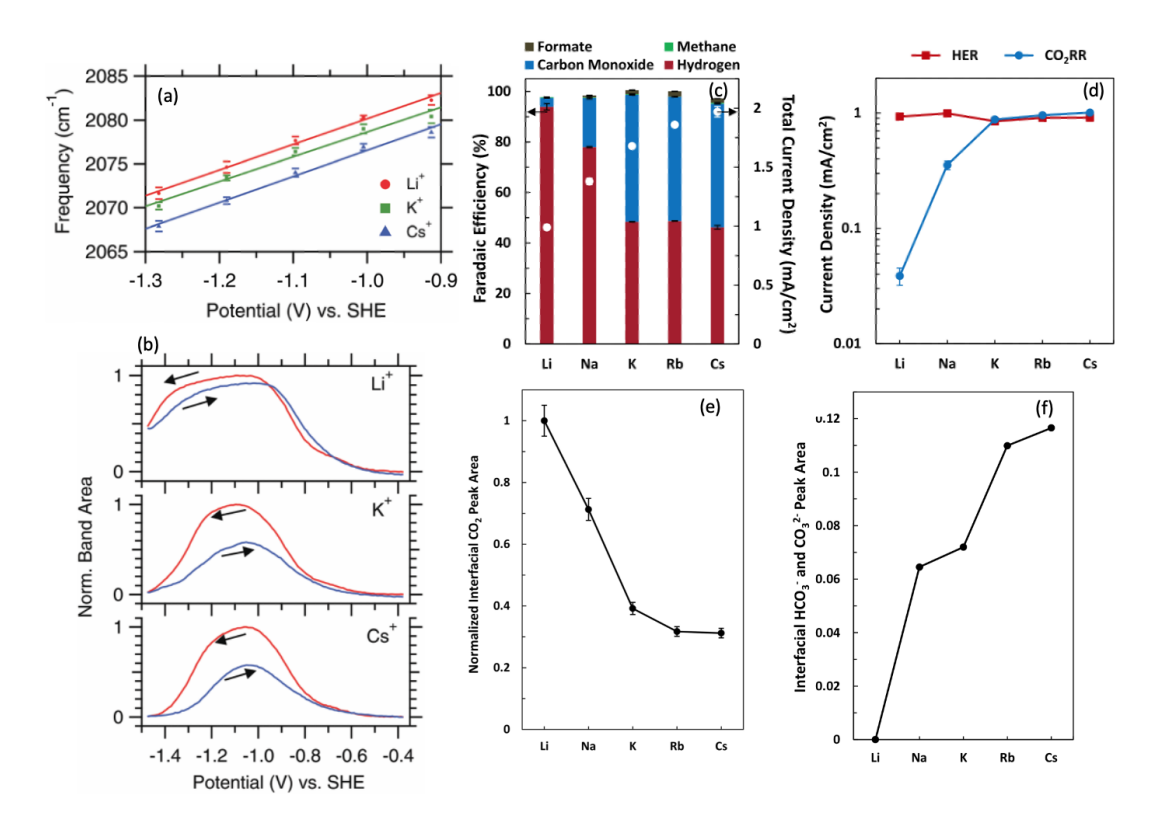


Fig. 8. Cation-dependent interfacial properties obtained by ATR-SEIRAS along with the selectivity and activity data in CO2ER; a) C≡O peak frequencies, and b) normalized peak area of CO as a function of potential in the electrolytes with different cations on Cu; Effect of cation size on c) FE of main products on Au, d) the current density for HER and CO2ER, e) normalized peak area of CO2, and f) Interfacial bicarbonate and carbonate peak area. Figure 8a-b are reproduced from Gunathunge et al. Copyright (2017), with permission from The Royal Society of Chemistry⁸⁹. Figure 8c-f are reprinted with permission from Malkani et al. Copyright (2020) American Chemical Society⁹¹.

In similar research but in CO₂ reduction, Malkani et al. utilized ATR-SEIRAS to determine the effect of cation size on the product selectivity (Fig. 8c), local CO₂ concentration (Fig. 8e) and the interfacial pH at an Au electrode surface⁹¹. The local pH was determined by the peak area of

the carbonate band^{14, 91}. The carbonate band area is directly proportional to the local pH (Fig. 8f). They reported that larger cations have a lower local CO₂ concentration and higher pH⁹¹ (Fig. 8e), conflicting with what Singh had shown previously⁸⁶. Low CO₂ concentration for large cations was attributed to the high rate of CO₂ consumption (Fig. 8d) due to electrochemical (CO2ER reactions) or chemical reactions (reactions with hydroxyl ions) ⁹¹.

Cations have been also reported to enhance the electric filed in the interface^{24, 86, 87}. The enhanced electric field attracts CO₂ molecules toward the surface and reduce the activation energy to intermediates formation^{24, 86, 87}. Ringe et al. theoretically investigated the effect of cation size on interfacial electric field strength¹¹⁷. Similar to the study from Waegele's group⁸⁹, they showed that the interfacial electric filed is stronger in larger cations-containing electrolytes (Fig. 9a)¹¹⁷. This is attributed to the small solvation shell for large cations which causes high concentration of cations in OHP and the surface charge enhancement¹¹⁷. The enhanced electric field stabilized the key intermediates for the formation of C₂ porducts¹¹⁷.

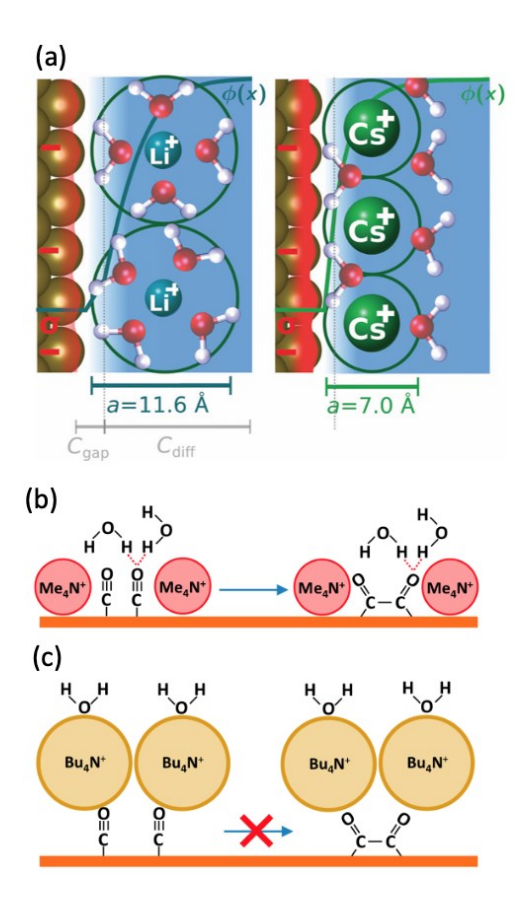


Fig. 9. Cation effect on the interfacial structure in CO2ER a) An illustration on how cation size affects the local cation concentration and the electric filed; Coupling mechanism of the adsorbed CO in b) methyl₄N⁺, and c) butyl₄N⁺. Figure 9a is reproduced with permission from Ringe et al. Copyright (2019), The Royal Society of Chemistry¹¹⁷. Figure 9b-c are reprinted with permission from Li et al. Copyright (2020) PNAS⁹⁰.

Although in many studies, researchers believe that cations cannot directly adsorb on the surface, Gao et al. showed that the presence of subsurface oxygen can make cations strongly adsorb to the surface¹²². Increasing the size of cation along with the subsurface oxygen will further stabilize the intermediate and enhance the FE for C_2 (69%)¹²².

So far, we have mainly focused on the studies on alkali cations, however there are also many research investigations which have reported the positive impact of other types of cations such as multivalent cations or IL cations in CO2ER.

Multivalent cations such as La³⁺ have been reported to enhance electrochemical reactions^{112,} ¹¹³, including CO2ER on a Cu-Sn-Pb alloy¹¹¹. Researchers showed a doubled CO2ER rate for La³⁺ electrolyte (LaCl₃) compared to Na⁺ electrolytes (NaCl) likely due to the high surface charge of La³⁺ which causes the CO₂⁻⁻ to polarize and facilitates the reduction¹¹¹.

Since CO is a key intermediate in CO₂ reduction, the studies on the effect of the cations in CO reduction can be also very helpful for the research on CO₂ reduction. In one such study on CO reduction, Li et al. used several bulky alkyl ammonium cations (100 mM) with different ionic radii (0.1 M methyl₄ N⁺, ethyl₄ N⁺, propyl₄ N⁺, butyl₄ N⁺ with borate (BO₃³⁻) as anion)⁹⁰. They showed the larger cations disrupted the interaction of CO and water at the interface and decreased the FE for ethylene⁹⁰. The results showed that by increasing the size of alkyl ammonium cations, the surface electric field decreased 90. This is because the larger cations cannot fit between the adsorbed CO90. Nonetheless, it was found that the effect of cation size on the electric field and on the CO adsorption is too small to play a significant role in decreasing the FE for ethylene. Therefore, the low FE for ethylene in the electrolytes with larger cations was not due to blocking the CO adsorption or due to the cation-dependent electric filed⁹⁰. The low FE_{ethylene} rather originates from disrupting the CO-water interactions which are necessary for ethylene formation (Fig. 9b-c)⁹⁰. Also, contrary to alkali cations, alkyl ammonium cations are not Lewis acids 90. Therefore, alkyl ammonium cations cannot buffer the local pH and also, they are unlikely to react with *CO which is a Lewis base. The large size of alkyl ammonium cations limits the chemical interaction with basic adsorbed CO and intermediates at the surface⁹⁰.

Using IL-based additives has recently attracted considerable attention due to their unique properties such as high CO₂ solubility and high stability in electrochemical experiments¹²³. The presence of ILs in the electrolyte has a vital influence in CO2ER¹²³. IL properties can be tuned by designing the IL structure such as increasing the cation chain length¹²³. Increasing the cation chain length enhances the IL hydrophobicity and CO₂ solubility ^{123, 124}. However, the bulkiness of the cation can reduce the stability of the cation-CO₂ complex which is formed during CO2ER and reduce the energy barrier^{123 25, 28}. The stability of the cation-CO₂ complex can be enhanced by the extra electron density on the ring¹²³. In this regard, Wu et al. investigated the effect of using a series of ILs with different cation chain lengths on CO2ER on lead¹²³. The results showed that a mixture of 1-benzyl-3-methylimidazolium tetrafluoroborate [Bzmim][BF₄] (14.17 wt.%)-water (11.7 wt.%)-acetonitrile can produce formate with 95.5% FE¹²³. This observation was attributed to the optimum hydrophobicity and the ability of the IL to stabilize the intermediates, and the optimum interactions between electrode/CO₂/IL¹²³.

Table 3. Selected examples of CO₂ reduction in aqueous electrolytes containing additives with different cations.

Additive	Main electrolyte	Catalyst	Example potential	Current density (mA/cm²)	FE (%) for main products	Ref.
0.05 M Li ₂ CO ₃ 0.05 M Na ₂ CO ₃ 0.05 M K ₂ CO ₃ 0.05 M Cs ₂ CO ₃	1 mM CTAB/H ₂ O	Cu	-1.05 V vs. RHE	~1.1° (j _{HCOO-})° ~0.9 (j _{HCOO-}) ~0.6 (j _{HCOO-}) ~3.2 (j _{HCOO-})	~18% HCOO ⁻ ~11% HCOO ⁻ ~8% HCOO ⁻ ~27% HCOO ⁻	73
0.1 M LiHCO ₃ 0.1 M NaHCO ₃ 0.1 M KHCO ₃ 0.1 M CsHCO ₃	H ₂ O	Cu	-1.45 V vs. SHE -1.45 V vs. SHE -1.39 V vs. SHE -1.38 V vs. SHE	5	6.19 C ₁ /C ₂ ratio 4.27 C ₁ /C ₂ ratio 1.06 C ₁ /C ₂ ratio 0.534 C ₁ /C ₂ ratio	36
0.5 M LiHCO ₃ 0.5 M NaHCO ₃	H ₂ O	Cu	-1.85 V vs. SCE	N.R.°	4% C ₂ H ₄ 11% C ₂ H ₄	94

		1				
0.5 M KHCO ₃					14% C ₂ H ₄	
0.5 M CsHCO ₃					13% C ₂ H ₄	
0.5 M NH ₄ HCO ₃					0% C ₂ H ₄	
0.1 M LiHCO ₃	H ₂ O	Ag	-1.0 V vs. RHE	~1.5	59.1% CO	86
0.1 M NaHCO ₃				~1.75	68.4% CO	
0.1 M KHCO ₃				~3.5	82.9% CO	
0.1 M RbHCO ₃				~4.4	82.2% CO	
0.1 M CsHCO ₃				~5.0	80.3% CO	
0.1 M LiHCO ₃	H ₂ O	Cu	-1.0 V vs. RHE	~2	~0% C ₂ H ₄ , ~0% C ₂ H ₅ OH	86
0.1 M NaHCO ₃				~2.1	5.5% C ₂ H ₄ , ~1% C ₂ H ₅ OH	
0.1 M KHCO ₃				~3	10.2% C ₂ H ₄ , ~2% C ₂ H ₅ OH	
0.1 M RbHCO ₃				~4	24.4% C ₂ H ₄ , 9.6% C ₂ H ₅ OH	
0.1 M CsHCO ₃				~4.5	31.1% C ₂ H ₄ , 11.4% C ₂ H ₅ OH	
0.1 M LiHCO ₃	H ₂ O	Ag	-1.0 V vs. RHE	~0.9 (j _{CO})	N.R.	87
0.1 M NaHCO ₃	_			~1.3 (jco)		
0.1 M KHCO ₃				~3 (j _{co})		
0.1 M RbHCO ₃				~4 (j _{CO})		
0.1 M CsHCO ₃				~5 (jco)		
0.1 M LiHCO ₃	H ₂ O	Sn	-1.0 V vs. RHE	~1.6 (j _{HCOO-})	N.R.	87
0.1 M NaHCO ₃				~2.2 (j _{HCOO-})		
0.1 M KHCO ₃				~2.8 (j _{HCOO-})		
0.1 M RbHCO ₃				~3 (j _{HCOO-})		
0.1 M CsHCO ₃				~3.1 (j _{HCOO-})		
0.1 M LiHCO ₃	H ₂ O	Cu	-1.0 V vs. RHE	~2.5	~10% C ₂ H ₄	87
0.1 M NaHCO ₃	2	(100)		~3	~17% C ₂ H ₄	
0.1 M KHCO ₃				~4	~25% C ₂ H ₄	
0.1 M RbHCO ₃				~3.9	~30% C ₂ H ₄	
0.1 M CsHCO ₃				~6	~40% C ₂ H ₄	
0.5 M NaCl	1.5 M HCl	Cu-Sn-	-0.65 V vs.	18.23 (C) ^d	28.2% CH ₃ OH,	111
		Pb alloy	Ag/AgCl		27.6% НСООН,	
					2.6% CH ₃ CHO	
0.166 M MgCl ₂				19.11 (C) ^d	34.1% CH ₃ OH,	
					23.6% HCOOH,	
0.166 M CaCl ₂				19.87 (C) ^d	2.3 % CH ₃ CHO 29.6% CH ₃ OH,	
0.100 IVI CaCI2				19.07(C)	25.8 HCOOH,	
					3.2 % CH ₃ CHO	
0.166 M BaCl ₂				20.55 (C) ^d	36.3% CH₃OH,	
					25.2% НСООН,	
					4.5% CH ₃ CHO	
0.08 M AlCl ₃				21.80 (C) ^d	17.8% CH ₃ OH,	
					28.4% НСООН,	

					7.20/ CH CHO	
0.08 M NdCl ₃				30.66 (C) ^d	7.3% CH ₃ CHO 34.6% CH ₃ OH, 24.2% HCOOH, 2.1 % CH ₃ CHO	
0.08 M LaCl ₃				34.11(C) ^d	35.7% CH ₃ OH, 24.5% HCOOH, 1.8% CH ₃ CHO	
0.33 M ZrCl ₄				22.68 (C) ^d	23.7% CH ₃ OH, 24.8% HCOOH, 17.6% CH ₃ CHO	
Blank	0.5 M	Ag	-1.6 V vs. SCE	~2.5	~50% CO	33
20 mM TTAB	NaHCO ₃			N.R.	~86% CO	
20 mM DTAB				~4	~95% CO	
20 mM DeTAB				N.R.	~82% CO	
20 mM OTAB				N.R.	~61% CO	
20 mM TMAB				N.R.	~54% CO	
20 mM NaBr				N.R.	~52% CO	
0.5 M NaHCO ₃	H ₂ O	Sn	-2.0 V vs. SCE	~10	~35% HCOO-	38
0.5 M KHCO ₃				~28	~63% HCOO-	
0.5 M CsHCO ₃				~30	~23% HCOO-	
0.5 M Na ₂ SO ₄	H ₂ O	Sn	-1.7 V vs. SCE	~5	~75% HCOO-	38
0.5 M K ₂ SO ₄	. 1120		11,7 1 151 2 2 2	~5	~40% HCOO	
0.5 M Cs ₂ SO ₄				~10	~20% HCOO-	
1 M NaCl	H ₂ O	Ag	-1.62 V vs.	80	75.0% CO	24
1 WI NaCI	П2О	Ag	Ag/AgCl	80	73.0% CO	
1 M KCl			-1.92 V vs.		95.6% CO	
	ii.		Ag/AgCl			
1 M RbCl			-1.88 V vs.		93.6% CO	
			Ag/AgCl			
1 M CsCl			-1.86 V vs. Ag/AgCl		87.0% CO	
1 M NaBr	H ₂ O	Ag	-1.84 vs. Ag/AgCl	80	60.8% CO	24
1 M KBr			-2.37 vs. Ag/AgCl		96.6% CO	
1 M RbBr			-1.79 vs. Ag/AgCl		95.8% CO	
1 M CsBr			-1.83 vs. Ag/AgCl		93.6% CO	
1 M NaI	H ₂ O	Ag	-1.67 vs. Ag/AgCl	80	80.8% CO	24
1 M KI			-1.89 vs. Ag/AgCl		96.6% CO	
1 M RbI			-1.70 vs. Ag/AgCl		96.5% CO	
1 M CsI	•		-1.65 vs. Ag/AgCl		101.7% CO	
1 M NaOH	H ₂ O	Ag	-1.62 vs. Ag/AgCl	80	83.0% CO	24
1 M KOH	. 2 -	8	-1.88 vs. Ag/AgCl		96.7% CO	
1 M RbOH			-1.72 vs. Ag/AgCl		91.6% CO	
1 M CsOH			-1.65 vs. Ag/AgCl		89.8% CO	
1 111 00011			1.00 .5.716/11601		02.070 00	

4. Non-ionic additives

Although most of the additives used in heterogenous CO2ER have an ionic nature, non-ionic organic additives such as primary amines and pyridine have been also used to enhance CO2ER (Table 4)¹²⁵⁻¹²⁸. Nitrogen-containing heterocyclic compounds such as pyridine have been reported to decrease the overpotential and promote CO2ER^{126, 127, 129}. Bocarsly's group showed that methanol can be produced with 22% FE on hydrogenated Pt and Pd electrodes in an aqueous electrolyte (0.5 M KCl) containing 10 mM pyridine¹²⁷.

Albo et. al. investigated the effect of pyridine additives in 0.5 M KHCO₃ on the activity and selectivity of Cu₂O-ZnO catalyst¹²⁸. They showed that the properties of the substitutes of the pyridine ring play an important role¹²⁸. By adding pyridine-based additive to the electrolyte, the overpotential for CO₂ electroreduction decreased. For example, a 200 mV decrease in overpotential was observed for 2-methylpyridine which has an electron donating group¹²⁸. They believe that the electron donation group facilitates the electron transfer and intermediate formation¹²⁸. Also, they reported that 10 mM 2- methylpyridine can enhance FE for methanol from 1.2% to 16.86%¹²⁸.

In another study, Abdinejad et al. reported that ethylenediamine (EDA) can significantly increase the CO FE% to 58% on Cu catalysts¹²⁵. They showed that amino groups undergo protonation in aqueous electrolytes and produce -NH₃⁺¹²⁵. -NH₃⁺ groups increase the solubility of the CO₂ by enhancing Lewis acid-base interactions¹²⁵.

^a Values with ~ have not mentioned in the original article but derived from the graphical results.

^b j: Partial current density for a specific product, not total current density.

^c N.R.: Not reported in the article.

^d Total charge (C) for 120 mins electrolysis. Current density values were not reported.

Table 4. Selected examples of non-ionic additive-containing aqueous electrolytes used for CO₂ reduction on different metals.

Additive	Main electrolyte	Catalyst	Potential	Current density (mA/cm ²)	FE (%) for main products	Ref.
Blank	0.1 M	Cu	-0.78 V vs.	4.7	1.1% CO	125
0.1 mM MEA	NaClO ₄ /		RHE	14.8	22% CO	
0.1 mM EDA	H ₂ O			18.4	58% CO	
0.1 mM DA				9.7	19% CO	
10 mM Pyridine	0.5 M KCl/ H ₂ O	Hydrogenated Pt and Pd	N.R.ª	0.05	22 ± 2 % CH ₃ OH, 10.8 ± 0.5% HCOOH	127
10 mM 4-tert- butylpyridine					14.5 ± 2 % CH ₃ OH, ~0 % HCOOH	
Blank	0.5 M KHCO ₃ /	Cu ₂ O/ZnO	-1.35 V vs. Ag/AgCl	1	1.2% CH ₃ OH	128
10 mM 2- methylpyridine	H ₂ O		-1.03 V vs. Ag/AgCl		16.86% CH₃OH	
25 mM 2- methylpyridine			-1.12 V vs. Ag/AgCl		11.44% CH ₃ OH	
50 mM 2- methylpyridine			-1.00 V vs. Ag/AgCl		8.43% CH₃OH	

^a N.R.: Not reported in the article.

5. Ions at the interface

Since CO₂ electroreduction is an interfacial phenomena-driven process, a deep understanding of the electrode/electrolyte interface is crucial to improve it. The interfacial structure is an important factor in electrochemical reactions since it can affect the diffusion of species, adsorption of reactants, charge transfer and the active site availability on the surface¹³⁰.

Even in diluted aqueous electrolytes, additive ions/molecules play a key role in the interfacial structure because they accumulate in the boundary layers around the charged electrodes. Depending on the structural and intrinsic properties of the ions/molecules in the electrolyte, electrode material, and electrode potential, various interfacial structures can be created in vicinity of the charged electrode. As mentioned earlier, the structure at the interface can alter CO₂ and

water, as reactants, concentration on the surface and also impact the formation of intermediates in CO2ER. Although the surface potential in CO2ER is much more negative than PZC of the metal electrodes, several studies have shown that adsorption of anions, in addition to cations, such as halides or dicyanamide can occur on even negatively charged metals during CO2ER. The presence of anions at the interface can positively or negatively, depending on the intrinsic properties of the anion, impact CO2ER. For example, it was shown that adsorption of Cl⁻ anions on Au enhanced CO formation, however, adsorption of H₂PO₄ on the same electrode enhanced HER due to its low pK_a⁵⁹. In the case of cations, it has been reported that the concentration of cations on the surface is directly proportional to the size of the hydration shell around the cations 86. Larger cations have a smaller hydration shell due to their lower surface charge density¹³¹. The small hydration shell causes the concentration of large cations to be higher at the interface compared to small cations ¹³¹. In addition to the effect of specifically adsorbed cations on the OHP potential and local pH which was discussed in the previous section, adsorbed cations can interact with CO₂ or intermediates on the surface. Similar to the anions, the presence of the cations on the surface can favor or disfavor formation of a certain product. For example, it has been shown that large cations decrease ethylene formation in CO reduction by disrupting the interactions of adsorbed CO with water on the surface⁹⁰ (Figure 9C).

In IL-containing electrolytes, different models have been proposed for the interactions of ions-CO₂-electrode on the surface (Figure 10). It needs to be mentioned that although some of these models have been proposed for the concentrated IL electrolytes or in the presence of organic solvents, they can still hold true, to some extent, in diluted aqueous solutions.

Some researchers believe that the cations of ILs on the surface react with CO₂ to create a complex between the cation and CO₂ (Eq. 1). This complex decreases the energy barrier to form

the radical intermediate and enhance CO2ER^{28, 132}. However, in a study using 0.1 M [Emim][NTF2] in acetonitrile, Sun et al. proposed a mechanism in which the adsorbed CO2 radical is stabilized by Emim⁺ cations on the surface (Fig. 10-a)¹³³. They showed that ILs can immobilize CO2 ⁻⁻ radicals at the surface, inhibit dimerization and reduce oxalate formation¹³³. By increasing the concentration of [Emim][NTF2], the CO dimerization to produce oxalate decreases and CO formation increases ¹³³. C2 position in imidazolium-based ILs has been reported as a key position for stabilizing the CO2 ⁻⁻ radicals in CO2ER ¹³⁴⁻¹³⁶ (Fig. 10-b). However, in a report using 0.02 M imidazolium salts in 1 M tetrabutylammonium hexafluorophosphate [TBA][PF6] in anhydrous acetonitrile, Lau et al. reported that the hydrogen bond between C4 and C5 of the imidazolium cations with CO2 ⁻⁻ plays the key role in providing high current densities in imidazolium -based electrolytes¹³⁷(Fig. 10-c).

EMIM
$$^{+}_{(ad)} + BF_{4}^{-} + CO_{2} + e^{-} \rightarrow [EMIM-CO_{2}]_{(ad)} ---- BF_{4}^{-} \rightarrow CO$$
 Eq. 1

Although the stabilization of adsorbed CO₂ molecules on the surface may be also due to the strong electric filed created by the hydrated cations on the surface ^{71, 138} (Fig. 10d), some studies showed that imidazolium cations are not always positively charged on the surface and may be reduced during CO2ER^{60, 61, 136, 139, 140}. In another mechanism proposed by Wang et. al., [Emim]⁺ cations first are reduced to [Emim] radicals and then create a complex with CO₂ molecules to form Emim-COOH and finally release CO¹³⁶ (Fig. 10e).

Although ILs are known to be stable in a wide range of potentials, the presence of the water can narrow their potential window. It has been reported that reduced adsorbed imidazolium molecules on the surface are the active sites for CO2ER¹³⁹. Wang et. al. showed that the

imidazolium cations are reduced in the presence of water at a less negative potential than expected¹³⁹. They showed that the reduction of imidazolium cations and CO₂ molecules occurred at the same potential (~-0.8 vs. SHE). This observation indicated that the adsorbed reduced imidazolium species as well as adsorbed cations have a significant contribution in CO2ER process¹³⁹.

In addition to the experimental research, a DFT study for CO2ER on Ag in an electrolyte containing 20 mol% [Emim][BF4] in water also revealed that the IL/water electrolytes have a lower overpotential for CO formation on Ag compared to the IL-free electrolytes¹⁴¹. An optimal solvation environment at the surface is created in the presence of ILs which can stabilize *COOH¹⁴¹. It was reported that a water molecule adsorbs to the *COOH intermediate in both IL-added and IL-free electrolytes. In the IL/water mixture, a multilayer consisting of water-anion-cation is created around *COOH intermediate and makes cations directly adsorb to the surface (Fig. 10f) ¹⁴¹. This phenomenon results in the metal electrons polarization toward the intermediate, enhancement of the electric field at the interface and consequently, the stabilization of *COOH intermediates such as *CO. It was also revealed that the IL-free aqueous electrolytes or for other intermediates such as *CO. It was also revealed that the IL-water mixture have a reduced entropy cost due to the limited motion of water molecules in the presence of ILs¹⁴¹.

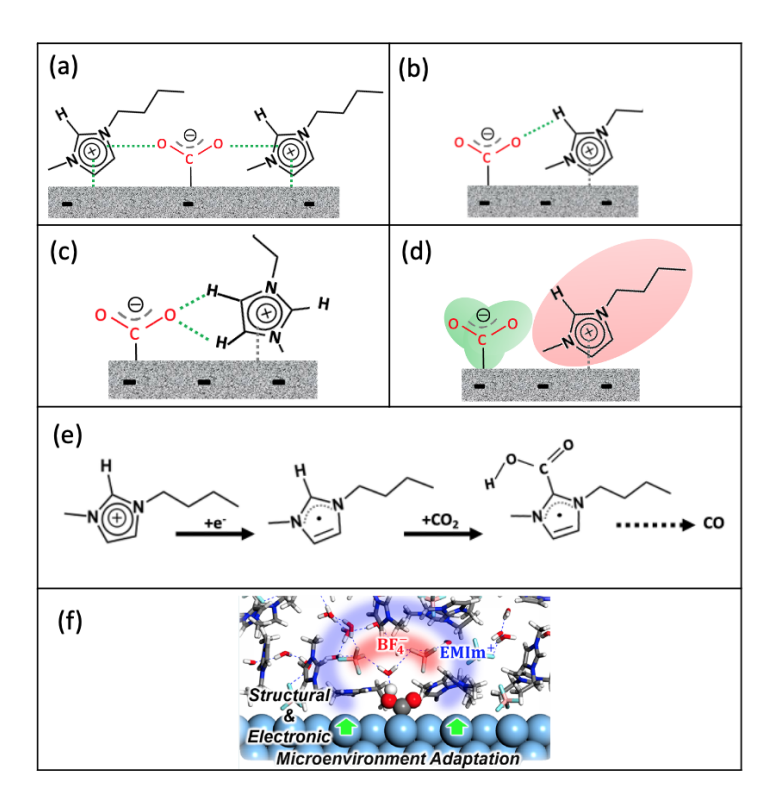


Fig. 10. Proposed mechanisms for the interaction of CO₂ with imidazolium-based ILs during CO2ER. a) stabilization of CO₂ with neighboring adsorbed cations; b) stabilization of CO₂ through hydrogen at C₂ position; c) stabilization of CO₂ through hydrogens at C₄ and C₅ positions; d) stabilization of CO₂ by local electric field created by cations at the interface; e) interaction of CO₂ with reduced imidazolium cation to produce CO; f) interfacial molecular structure proposed in a 20:80 [Emim][BF₄]- water electrolyte over Ag electrodes. Figure 10f is reprinted with permission from Lim et al. Copyright (2018) American Chemical Society¹⁴¹.

Regarding the orientation of ions on the surface, [Bmim]⁺ cations are less flexible compared to the bulky anions such as NTF₂ due to their planar structure which has a well-defined polar and nonpolar regions¹⁴². So, [Bmim]⁺ can more effectively screen the surface¹⁴².

Potential is another factor affecting the interfacial structure and the orientation of additives¹⁴³, ¹⁴⁴. It has been reported that the orientation of [Bmim]⁺ cations on Cu surface is a function of potentials. By going to more negative potentials, the orientation of [Bmim]⁺ cations changes from a vertical to a flat configuration to maximize the attractive interaction with the surface (Fig. 11)¹⁴⁴, ¹⁴⁵. The onset potential for the configuration change of the [Bmim]⁺ cation depends on the nature of the anions¹⁴⁴. The alkyl chain length in imidazolium-based ILs also influence the adsorption of cations and the thickness of double layer. It has been observed that increasing the alkyl chain length enhances the adsorption ability of the cations and reduce the thickness of the double layer¹³⁰,



Fig. 11. Dependance of the IL orientation to the electrode potential. Reproduced with permission from Yuan et al. Copyright (2010) Wiley¹⁴⁴.

6. Water molecules on the surface

The electrode polarization not only impacts the ion configurations, it also influences the water molecule adsorption due to the dipole moment of water¹⁴⁷. Theoretical studies show that water molecules are accumulated at the charged surface¹⁴⁷. The presence of the water in the interface as a hydrogen source can affect CO2ER^{28, 148}. Several factors such as electrolyte composition, electrolyte concentration, electrode material, and electrode potential significantly impact the water molecules concentration and structure at the interface.

Feng et al. have reported that water molecules are condensed in the interface of [Bmim][PF6] and the carbon electrode¹⁴⁷. The accumulation of water molecules is more pronounced on the positive electrode, where the anions are dominant in the interface, compared to the negative electrode^{147, 149}. This is because of the stronger interaction of water with anions compared to cations. The water condensation also decreases the coulombic interaction between ions and ions-electrode¹⁴⁹.

It has been revealed that the structure of interfacial water is significantly different from that in the bulk. The water orientation is dependent on the electrode potential. While at negative surfaces, the water molecules weakly bind to the surface from hydrogen side, the water molecules have a strong interaction with positively charged surface from their oxygen atom that makes them to have a nearly flat orientation on the surface^{150, 151}.

In one of our recent studies, it was also observed that the anion hydrophilicity in the electrolyte can impact CO2ER by altering the water concentration at the surface⁴¹. It was shown that hydrophilic [DCA]⁻ anions which have a high affinity to adsorb on the surface, significantly enhanced HER due to adsorbing water molecules and repelling CO₂ from the surface⁴¹.

In one study, the interfacial water in an electrolyte containing 0.1 M NaHCO₃ and 67 μM CTAB was investigated by attenuated total reflectance surface-enhanced infrared absorption spectroscopy (ATR-SEIRAS) ¹⁵². Results showed that the interfacial water concentration decreased by adding CTAB to the electrolyte due to the water displacement by bulky hydrophobic CTAB¹⁵². The water replacement was also the reason for HER suppression in the presence of CTAB¹⁵².

7. Techniques to study the interface

Different techniques have been used to study the molecular structure at the interface in electrochemical reactions. The following techniques are the most frequently used methods which can provide information on the nature of molecular species and their orientations on the surface.

7.1. Cyclic voltammetry (CV)

CVs in CO₂-free electrolytes can provide useful information about HER. In a research conducted on the effect of IL in CO2ER, CVs in Ar-saturated electrolytes showed that by adding IL to the electrolyte, a negative shift for the HER onset potential was observed ¹³⁹ (Fig. 12). This negative shift was attributed to a layer of cations formed by the interaction of Cu electrode and IL¹³⁹. Study of the second cycles of CVs also showed interesting results¹³⁹. There was no difference between the 1st and 2nd cycles for IL-free electrolytes, however, a negative shift was observed for the second scan in IL-added electrolytes¹³⁹. This observation was attributed to reduction of IL cations at the Cu surface¹³⁹. The same observations were not observed for the glassy carbon (GC) which indicates the unique interaction of Cu and ILs¹³⁹. There is a very small difference between the first and second scan of the CVs in CO₂-saturated electrolytes which shows that the layer formed during the scan does not block CO2ER¹³⁹. The interaction of IL with the Cu electrode was also found by a shoulder observed in Ar- saturated electrolyte¹³⁹. An oxidation peak at -0.2 V was also observed in Ar-saturated IL-added electrolyte which can be attributed to the oxidation of reduced cation¹³⁹. However, this oxidation peak was not observed in the presence of CO₂, likely due to the reaction of CO₂ with reduced IL¹³⁹.

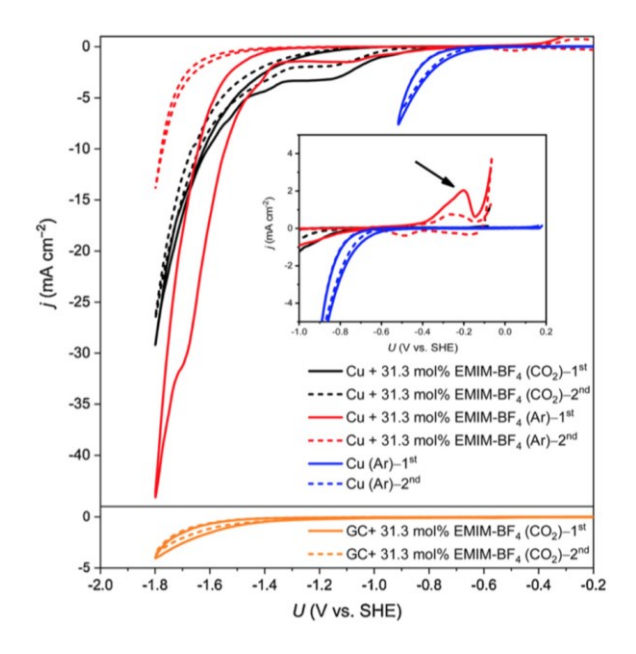


Fig. 12. The first and second scans of CVs of Cu and GC in different electrolytes.

Dependance of the IL orientation to the electrode potential. Reprinted from Wang et al.

Copyright (2020), with permission from Elsevier¹³⁹.

7.2. Electrochemical impedance spectroscopy (EIS)

Another useful technique to study the electrolyte-electrode interface is electrochemical impedance spectroscopy (EIS). In a study conducted by Verma et. al. EIS was used to provide an insight into the influence of electrolyte concentration and anion nature in CO2ER²². They showed that increasing the KOH concentration from 0.5 to 3 M in the aqueous electrolytes, decreased the solution and charge transfer resistance²². The decrease in solution resistance was attributed to the improved conductivity in more concentrated KOH electrolyte²². The lower charge transfer resistance for 3 M KOH was explained by the enhanced ability of the cations to stabilize the radical CO₂ intermediates²². Given the EIS data for different anions (2 M KOH, KHCO₃, KCl), charge transfer resistance changed in the following order KOH < KHCO₃ < KCl²². They believe that

several factors such as local pH, specific adsorption ability, and conductivity are responsible for this observation²². For example, Cl⁻ anions which strongly adsorb to the surface, destabilize the intermediate and lead to suppress CO2ER²².

EIS can also be used to determine the double layer capacitance (C_{dl}). In a research on the effect of 1 mM CTAB on the interfacial structure in different electrolytes (0.05 M Li₂CO₃, Cs₂CO₃), the double layer capacitance was measured by EIS⁷³. It was found that C_{dl} for all electrolytes in the absence of CTAB is almost the same⁷³. However, C_{dl} for Cs⁺-containing electrolytes is higher than Li⁺ electrolytes in the presence of CTAB⁷³. The authors believe that hydrated Li⁺ can be displaced by CTAB, while CTAB cannot displace the Cs⁺ layer on the surface. Therefore, the interfacial concentration of the cations and C_{dl} are higher in Cs⁺ solutions compared to Li⁺ ⁷³.

7.3. In-situ Raman

In-situ Raman spectroscopy is a powerful technique to gain the information about the species at the surface during electrolysis. Wang et al. studied the CO2ER on a copper electrode by in situ Raman at different potentials to indicate the importance of the reduced imidazolium cation layer in CO2ER¹³⁹. The results showed the structural change of imidazolium by changing the potential¹³⁹ (Fig. 13a). A new band appeared after -1 V vs. SHE at 1252 cm^{-1 139}. This observation showed the formation of the reduced imidazolium- CO₂ complex at potentials more negative than -1 V, the protentional where CO2ER also initiates¹³⁹.

In another study, Santos et al. employed the surface enhanced Raman scattering (SERS) to study the CO2ER on Cu surface in [Bmim][BF₄]¹⁵³. They reported that the presence of different species on the surface such as adsorbed CO, CO₂, [Bmim]⁺-CO₂ complex and [Bmim] carbene can be confirmed by SERS¹⁵³. CO₂ signals in SERS shifted to a lower frequency (2275 cm⁻¹) compared

to the gas CO₂ signal which indicates the adsorption of CO₂ to the Cu surface¹⁵³. At lower overpotentials, the CO signal was assigned to the adsorbed CO on Cu₂O. At very high negative potentials, the signals for CO molecules adsorbed on Cu₂O film disappeared and new signals for CO (adsorbed on different active sites on Cu), C=C bonds and carboxylate appeared¹⁵³. This observation indicated the presence of Bmim-CO₂ complex on the surface¹⁵³. The results suggest that the Cu/Cu₂O electrodes can be used in IL-based electrolytes for CO2ER at low overpotentials¹⁵³.

7.4. Sum frequency generation (SFG)

SFG can be employed to explore the mechanism of CO2ER. SFG is able to detect the produced and adsorbed species such as CO on metals¹³². By using SFG, researchers showed that accumulation of CO poisons Pt electrodes¹³² but it does not poison the Ag surface¹⁵⁴. It has been also reported that the intensity of adsorbed CO and CO₂ is dependent on the potential. Rosen et al. used SFG to show that imidazolium cations form a layer of CO₂-Emim complex at E<-1 V which inhibits HER but enhances CO2ER on Pt¹³² (Fig. 13b). The complex is then converted to CO. By going toward more negative potentials, a new peak was observed at 2348 cm⁻¹ which is indicative of CO₂-containing species¹³². This peak cannot be attributed to the free bulk CO₂,which is not SFG-active or the adsorbed CO₂ which appears in a much lower frequencies¹³². Therefore, this peak is assigned to the CO₂-Emim complex¹³².

Rey et al. also studied the interfacial structure of [Emim][BF4] on Ag as a function of potential in CO2ER by non-resonant SFG¹⁵⁴. The signal intensity versus potential curve showed a minimum at the same potential as the threshold potential for CO2ER (-1.33 V vs Ag/AgCl) ¹⁵⁴. The location of this minimum was independent of the presence of CO₂ and was a characteristic of the IL itself¹⁵⁴. The curvature increased after the minimum point toward the more negative potentials which

indicates the structural transition of the ILs in the double layer¹⁵⁴. An increased Stark shift for adsorbed CO at the threshold potential was also observed which was attributed to the enhanced interfacial electric field at this potential¹⁵⁴. The coincidence of the structural transition of ILs and the enhancement of the electric field with starting the CO2ER indicates that the IL structural transition control CO2ER¹⁵⁴. Also, the results showed that CO weakly adsorb on Ag and therefore, CO doesn't poison the Ag surface¹⁵⁴.

In another study, Kemna et al. have recently used SFG to study the water structure on Pt surface in the presence of [Emim][BF4]¹⁵⁵. O-H and C-H modes were used to analyze the water structure (Fig. 13c-e) and the orientation of [Emim]⁺ cations at the surface as a function of potential, respectively¹⁵⁵. SFG showed that the structure of water molecules in the bulk and at the interface is significantly different (Fig. 13f) ¹⁵⁵. While water molecules are in the form of free and isolated molecules in the bulk (3560 and 3645 cm⁻¹), the water molecules at the interface create a layer (3400 cm⁻¹) consisting of hydrogen-bonded molecules which grow by increasing the overpotential¹⁵⁵. The change in C-H band was also attributed to the change of cation orientation on the surface by potential¹⁵⁵.

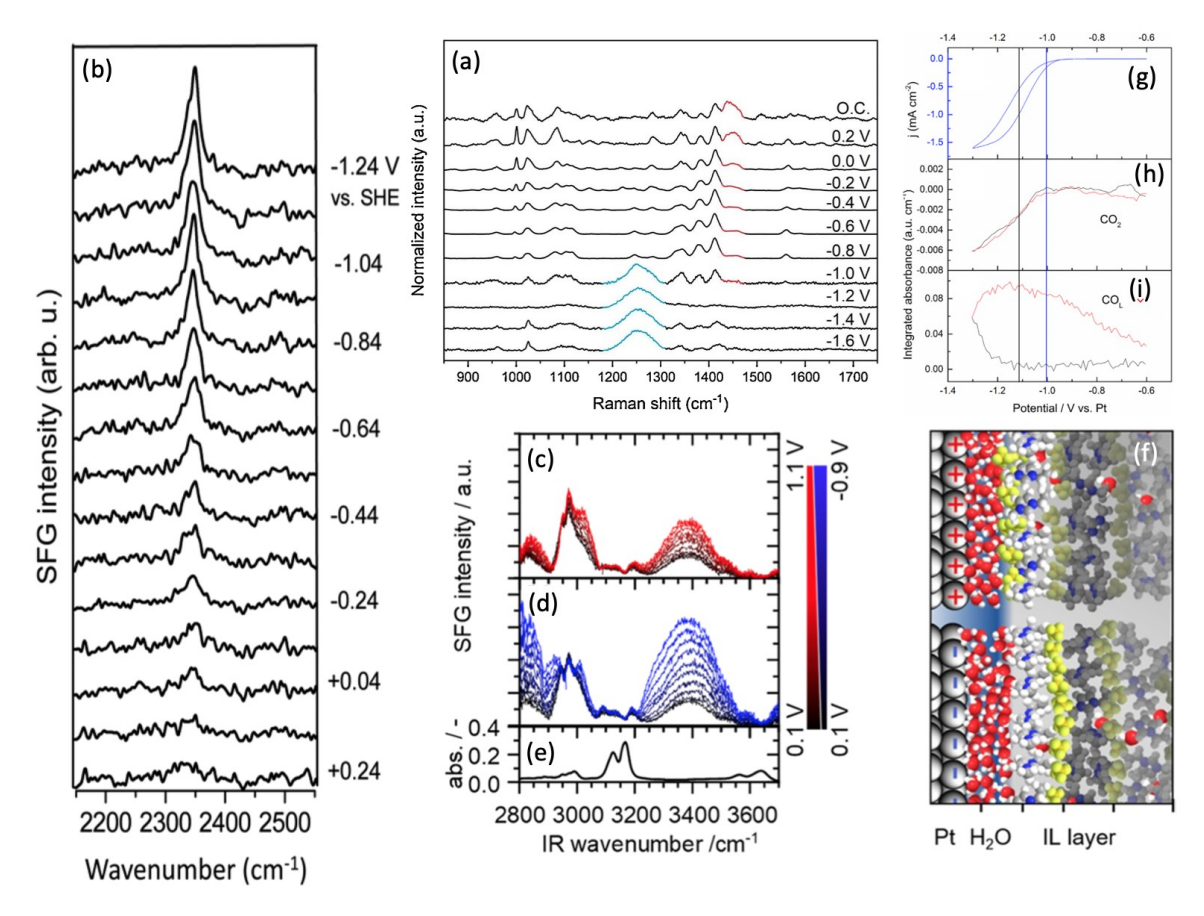


Fig. 13. Interfacial data obtained by spectroscopic techniques at different potentials in IL/water mixtures; a) Raman spectra obtained on Cu in 100 mM [Emim][BF4] aqueous solution at different potentials; b) SFG spectra measured in [Emim][BF4] containing 90 mM water at different potentials; SFG spectra of Pt in [Emim][BF4]/H2O electrolyte at c) E>0.1 V, d) E< 0.1 V, e) IR absorbance spectra for IL/water electrolyte, and f) structure of IL-water-Pt surface; g) CVs and the integrated absorption of CO₂ (h) and CO_L (i) as a function of the potential. Figure 13a is reprinted from Wang et al. Copyright (2020), with permission from Elsevier¹³⁹. Figure 13b is reprinted with permission from Rosen et al. Copyright (2012) American Chemical Society¹³². Figure 13c-f are reprinted with permission from Kemna et al. Copyright (2020) American Chemical Society¹⁵⁵. Figure 13g-i are reprinted with permission from Papasizza et al. Copyright (2018) American Chemical Society¹²¹.

7.5. In situ attenuated total reflectance-surface enhanced infrared absorption spectroscopy (ATR-SEIRAS)

ATR-SEIRAS has been reported to estimate the interfacial CO coverage, CO₂/ HCO₃⁻ concentration, electric field and local pH^{89, 91, 116, 121}. The local pH is proportional to the HCO₃⁻/ CO₂ concentration ratio on the surface¹¹⁶. ATR-SEIRAS has been used in several studies to investigate the effect of alkali cation size on the interfacial pH and CO₂ concentration and different results have been obtained^{89, 91, 116}. Some researchers showed that larger alkali cations create a smaller HCO₃⁻/CO₂ concentration ratio and consequently lower pH at the interface¹¹⁶. However, it was recently shown that larger cations create a higher interfacial HCO₃⁻ concentration, higher local pH and lower CO₂ concentration due to the higher rate of CO₂ consumption by chemical surface⁹¹ electrochemical reactions the electrode (Fig. or at 8e-f). The source of this discrepancy is unclear, but it seems that there might be other factors (except local pH) such as the interfacial electric filed playing the key role in CO2ER. The interfacial electric field can be also estimated based on the frequency shift observed for C≡O band⁸⁹. Larger cations showed a stronger electric field at the surface⁸⁹.

In another research, ATR-SEIRAS and CVs were simultaneously used to study CO2ER on Au in [Emim][BF4]/H₂O mixture (18mol%)¹²¹. In the reductive scan in the CV, a decrease in the interfacial CO₂ concentration was detected when an increase in the reductive current in CV was observed¹²¹ (Fig. 13g-h). This can be due to the reduction of CO₂ to CO on Au¹²¹. The peak for adsorbed CO was appeared at a more negative potential probably due to its low concentration at the beginning step of the reduction¹²¹ (Fig. 13i). By comparing the spectra for CO₂- and CO-saturated solutions, it was found the interfacial structure is different¹²¹. In CO₂-saturated spectra,

there are two peaks for adsorbed CO (CO_L and CO_B), however, in CO-saturated solutions, a single broad peak at CO_L frequency was observed likely due to the lower coverage of CO_L which decreases the probability of dipole—dipole coupling of the adsorbed CO_{ad} molecules¹²¹. Moreover, by adding CO₂ to the IL/water mixture, a negative peak for Emim⁺ was observed at 1455 and 1575 cm⁻¹ ¹²¹. The intensity of [Emim]⁺ peak was enhanced by going to more negative potentials. This can show how the adsorbed CO produces from CO2ER can influence the surface charge density and the reorientation of [Emim]⁺. FTIR also revealed the presence of two types of water molecules on the surface¹²¹. The first type is bulk-like water with a high amount of hydrogen bonding and the second one is the water in interfacial IL-rich environment with a low degree of hydrogen bonding¹²¹. By adding CO₂ to the system, only bulk-like water is detected on the surface at negative potentials and the water in IL-rich environment is depleted from the surface likely due to its consumption in CO2ER as the proton source¹²¹.

7.6. Scanning tunneling microscopy (STM)

Scanning tunneling microscopy (STM) technology is another important method to study the electrochemistry of the surface at the level of atomic resolution. STM can be also employed to study the lateral species distribution and the potential-dependent catalyst morphology. Liu et. al. studied the adsorption of [Emim][NTF2] and [EMmim][NTF2] on Au by using STM¹⁵⁶. It was found that the Au surface was etched in the presence of [Emim][NTF2], however, no etching was found for [EMmim][NTF2]¹⁵⁶. They attributed this observation to the strong interaction of [Emim][NTF2] to Au¹⁵⁶. In another study, Gnahm et al. studied the interface of Au-[Bmim][PF6] interface with STM¹⁵⁷. They found the STM is not able to provide clear imaging at positive potentials probably due to the extra adsorption of the IL to the surface¹⁵⁷. It needs to be mentioned that STM is only useful to study the species which are directly adsorbed on the surface. However,

in order to study the adsorption behavior of species in the double layer, other techniques such as AFM can be used¹⁵⁶.

7.7. Atomic fore microscopy (AFM)

AFM has an ability to give insight on the thickness of multilayers and also the vertical distribution of species at the surface. Li et al. have employed AFM to investigate the effect of alkyl chain length in imidazolium-based cations and the nature of anions (FAP⁻ and I⁻) on the interfacial IL structure on the Au electrode as a function of potential¹⁵⁸. AFM showed the ILs create a multilayer structure at the interface¹⁵⁸. The interfacial layer is dominated by the counter ions which are strongly adsorbed to the Au surface¹⁵⁸. In opposite to FAP⁻ anions, I⁻ anions have a stronger interfacial structure at positive potentials compared to [Bmim]⁺ cations at negative potentials¹⁵⁸. Regarding the effect of the alkyl chain length, based on the forces to break the interfacial layers in AFM, 1-butyl-3-methylimidazolium [Bmim]⁺ showed the weakest structure¹⁵⁸. 1-Ethyl-3-methylimidazolium [Emim]⁺ and 1-hexyl-3-methylimidazolium [Hmim]⁺ both showed a strong layer in the interface. The parallel orientation of [Emim]⁺ allowed ILs to strongly adsorb to the surface¹⁵⁸. The long alkyl chain of [Hmim]⁺ also creates a well-defined interfacial structure due to the strong solvophobic forces between layers¹⁵⁸.

The effect of water concentration on the structure of the ionic liquid ([Emim][OTF])-Au interface have been also studied by AFM¹⁵⁹. The results showed that the interaction of the cationanion in ILs decreases by adding 30 vol % water to the electrolyte due to hydrogen bonds between cation-water and anion-water¹⁵⁹. The structure of the innermost layer not only relies on the applied potential, but it is also impacted by the water concentration in the electrolyte¹⁵⁹. At low concentration of water, the classical Gouy–Chapman–Stern theory doesn't hold true because of the multilayer nature of the interface¹⁵⁹. However, it was reported that the interfacial structure

changes from a multilayered to a double layered structure by going from 30% to 50% water content¹⁵⁹ (Fig. 14). They showed that similar to the diluted aqueous electrolytes with small ions, the electrolytes with more than 50% water has only one well-defined stern layer at the interface which is enriched by hydrated cations¹⁵⁹.

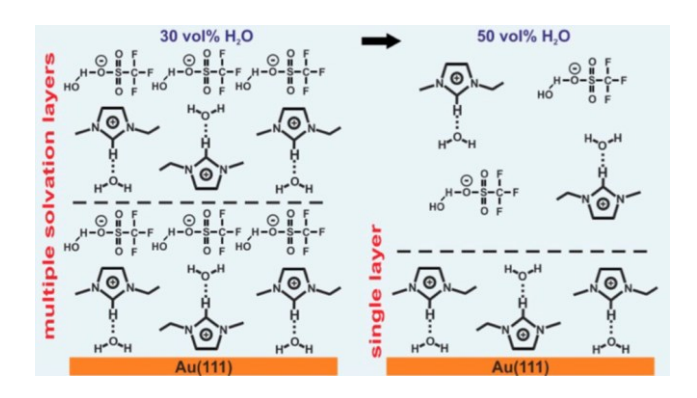


Fig. 14. The structure of the IL-water-Au interface in different water concentration.

Reprinted with permission from Cui et al. Copyright (2016) American Chemical Society¹⁵⁹.

7.8. X-ray photoelectron spectroscopy (XPS)

XPS can be used to investigate the presence of the species strongly adsorbed on the surface by analyzing the surface chemical composition. In our previous research, we also used XPS to analyze the Cu surface after CO2ER in different IL-added electrolytes. Among ILs studied in that research (10 mM [Bmim][X], X=Cl, Ac, NTF₂, OTF, DCA), [Bmim][DCA] showed the maximum amount of ILs adsorbed on the Cu surface which indicates the strong adsorption of DCA⁻ anions with the Cu during CO2ER ⁴¹. Feaster et. al. also used XPS to analyze the Cu, Ag, and Fe surface after HER in acid and basic conditions in the presence of 100 mM [Emim]Cl additive⁴². XPS showed that N and Cl were detected on all metal surfaces when using [Emim]Cl in acidic conditions⁴². However, in the basic electrolytes, only the metal and C peaks were observed⁴². This observation showed the strong interaction of IL with the metal surface in acidic solutions⁴².

7.9. Electrochemical quartz crystal microbalance (EQCM)

EQCM is also a powerful technique to study the adsorption behavior of species on the surface. In EQCM, the frequency shift (dF) due to adsorption/desorption of species or reduction/oxidation of the electrode can be measured and converted to the mass change (dM). the adsorption behavior of the molecules on the surface is highly dependent on the concentration of molecules. Ramírez-Cano et. al. used EQCM technique to investigate the adsorption of 2-mercaptobenzothiazole (2-MBT) at different concentrations (0.001 mM to 100 mM)¹⁶⁰. Based on the results obtained in this research, the authors proposed a mechanism for the adsorption of molecules on the surface 160. They suggested that 2-MBT molecules first come to the surface and displace the water molecules already adsorbed on the surface 160. After adsorption on the active sites of the surface, 2-MBT molecules rearrange on the surface and displace more water molecules around 160. Desorption of the water molecules provides more space for the 2-MBT molecules in the electrolyte to adsorb on the surface and consequently, cover the surface 160. The results showed that at concentrations above 1 mM, dM exponentially increases by time and followed the Langmuir adsorption isotherm 160. They attributed this observation to adsorption of a large number of 2-MBT molecules 160. However, in concentrations lower than 0.1mM, since the 2-MBT molecules cannot make up for the mass loss created by the water desorption, the desorption process dominates rather than 2-MBT molecules adsorption¹⁶⁰.

Medina-Ramos et. al. also used EQCM to study the bismuth-electrolyte interface during CVs in a CO₂-saturated 100 mM [Bmim][OTF]/MeCN solution¹⁶¹. The dF (frequency shift) and dR (resistance shift) obtained during CVs, showed a significant change in roughness and viscosity of the surface depending on the potential¹⁶¹. The change in frequency was attributed to the

adsorption/desorption of ions or oxidation/reduction of the electrode and the change in R was attributed to the interfacial viscosity or surface roughness¹⁶¹. By going toward more negative potentials, EQCM showed a mass loss followed by a mass gain¹⁶¹. The initial mass loss was attributed to the reduction of the electrode and the subsequent mass gain was related to the adsorption of IL to the surface¹⁶¹.

8. Challenges and future prospects

Aqueous electrolytes are still the most common electrolytes for practical CO2ER. However, new strategies need to be developed to enhance CO₂ solubilities, reduce HER, increase current density, and improve the selectivity in these electrolytes. In order to design an efficient CO2ER electrolyzer, a comprehensive understanding of the reaction mechanism is an urgent need. Although the crucial impact of the electrolyte is observed in CO2ER, the exact role of species in the electrolyte is still vague. A profound understanding on how the ions/molecules of the additives interact with each other, water, CO₂, intermediates, and the electrode surface during CO2ER can be helpful to design the system. There are still several questions and contradictory findings in the field which can be the topics for the future studies. For example, different opinions exist for the effect of cation size on the local pH and interfacial CO₂ concentration so far. Also, a comprehensive understanding of the CO2ER is not possible without developing in-situ characterization techniques to study the catalyst-electrolyte interface during CO2ER. The existing in-situ techniques also need to be improved to provide a stronger intensity for the intermediates with low coverage. Also, the combination of theoretical and experimental research in the field can be mutually beneficial and of interesting topics for future studies. Based on the knowledge obtained in this review paper, an efficient system to have a high selectivity for CO2ER should provide a high concentration of CO₂ at the surface, lower the interfacial water concentration and keep the local pH neutral during CO2ER. Hydrophobic additives with high CO₂ adsorption capacity can be a promising option for CO2ER. However, the solubility of hydrophobic additives in aqueous electrolytes is a concern which needs to be addressed.

Declaration of Competing Interest

The authors declare that they have no known competing financial interests or personal relationships that could have appeared to influence the work reported in this paper.

Acknowledgements

The financial support of the National Science Foundation (Grant No. 1935957) is appreciated.

Abbreviations

The following abbreviations have been used in this manuscript.

[Bzmim] 1-benzyl-3-methylimidazolium

[Bmpyrr] 1-butyl-1-methylpyrrolidinium

[Bmim] 1-butyl-3-methylimidazolium

[Emim] 1-ethyl-3-methylimidazolium

[Hmim] 1-hexyl-3-methylimidazolium

(2-MBT) 2-mercaptobenzothiazole

[Ac] Acetate

MeCN Acetonitrile

AAAS American association for the advancement of science

AFM Atomic fore microscopy

ATR-SEIRAS In situ attenuated total reflectance-surface enhanced infrared absorption

spectroscopy

HCO₃ Bicarbonate

[NTf₂] Bis(trifluoromethylsulfonyl)imide

BO₃ Borate

CO₃ Carbonate

CTAB Cetyltrimethylammonium bromide

ClO₄ Chlorate

CV Cyclic voltammetry

DA Decylamine

DeTAB Decyltrimethylammonium bromide

[DCA] Dicyanamide

DTAB Dodecyltrimethylammonium bromide

EDA Ethylenediamine

EIS Electrochemical impedance spectroscopy

EQCM Electrochemical quartz crystal microbalance

FE Faradaic efficiency

PF₆ Hexafluorophosphate

OH Hydroxide

IL Ionic liquid

MEA Monoethanolamine

Tolyl-pyr N-tolylpyridinium chloride

OTAB Octyltrimethylammonium bromide

OHP Outer Helmholtz plane

PO₄ Phosphate

PNAS Proceedings of the national academy of sciences of the united states of America

SO₄ Sulfate

SFG Sum frequency generation

STM Scanning tunneling microscopy

[TBA] Tetrabutylammonium

Butyl₄ N⁺ Tetrabutylammonium

Methyl₄ N⁺ Tetramethylammonium

Ethyl₄ N⁺ Tetraethylammonium

Propyl₄ N⁺ Tetrapropylammonium

TTAB Tetradecyltrimethylammonium bromide

BF₄ Tetrafluoroborate

TMAB Tetramethylammonium bromide

OTF Trifluoromethanesulfonate/Triflate

FAP Tris(pentafluoroethyl)trifluorophosphate

XPS X-ray photoelectron spectroscopy

- 1. Kuhl, K. P.; Cave, E. R.; Abram, D. N.; Jaramillo, T. F., New insights into the electrochemical reduction of carbon dioxide on metallic copper surfaces. *Energy Environ. Sci.* **2012**, *5* (5), 7050-7059.
- 2. Hori, Y., Electrochemical CO₂ reduction on metal electrodes. In *Modern Aspects of Electrochemistry*, Vayenas, C. G.; White, R. E.; Gamboa-Aldeco, M. E., Eds. Springer: New York, 2008; Vol. 42, pp 89-189.
- 3. Nguyen, D. L. T.; Kim, Y.; Hwang, Y. J.; Won, D. H., Progress in development of electrocatalyst for CO₂ conversion to selective CO production. *Carbon Energy* **2020**, *2* (1), 72-98.
- 4. Zhang, R. Z.; Wu, B. Y.; Li, Q.; Lu, L. L.; Shi, W.; Cheng, P., Design strategies and mechanism studies of CO₂ electroreduction catalysts based on coordination chemistry. *Coord. Chem. Rev.* **2020**, *422*.
- 5. Schouten, K. J. P.; Pérez Gallent, E.; Koper, M. T. M., The influence of pH on the reduction of CO and CO₂ to hydrocarbons on copper electrodes. *J. Electroanal. Chem.* **2014**, *716* (Supplement C), 53-57.
- 6. Ooka, H.; Figueiredo, M. C.; Koper, M. T. M., Competition between hydrogen evolution and carbon dioxide reduction on copper electrodes in mildly acidic media. *Langmuir* **2017**, *33* (37), 9307-9313.

- 7. Singh, M. R.; Clark, E. L.; Bell, A. T., Effects of electrolyte, catalyst, and membrane composition and operating conditions on the performance of solar-driven electrochemical reduction of carbon dioxide. *Phys. Chem. Chem. Phys.* **2015**, *17* (29), 18924-18936.
- 8. Nitopi, S.; Bertheussen, E.; Scott, S. B.; Liu, X.; Engstfeld, A. K.; Horch, S.; Seger, B.; Stephens, I. E. L.; Chan, K.; Hahn, C.; Nørskov, J. K.; Jaramillo, T. F.; Chorkendorff, I., Progress and perspectives of electrochemical CO₂ reduction on copper in aqueous electrolyte. *Chem. Rev.* **2019**, *119* (12), 7610-7672.
- 9. Yoon, Y.; Hall, A. S.; Surendranath, Y., Tuning of silver catalyst mesostructure promotes selective carbon dioxide conversion into fuels. *Angew. Chem., Int. Ed.* **2016,** *55* (49), 15282-15286.
- 10. Chen, C. Z.; Zhang, B.; Zhong, J. H.; Cheng, Z. M., Selective electrochemical CO₂ reduction over highly porous gold films. *J. Mater. Chem. A* **2017**, *5* (41), 21955-21964.
- 11. Ma, M.; Djanashvili, K.; Smith, W. A., Controllable hydrocarbon formation from the electrochemical reduction of CO₂ over Cu nanowire arrays. *Angew. Chem., Int. Ed.* **2016**, *55* (23), 6680-6684.
- 12. P. Schouten, K. J.; Gallent, E. P.; Koper, M. T. M., The electrochemical characterization of copper single-crystal electrodes in alkaline media. *J. Electroanal. Chem.* **2013**, *699*, 6-9.
- 13. Liu, X.; Schlexer, P.; Xiao, J.; Ji, Y.; Wang, L.; Sandberg, R. B.; Tang, M.; Brown, K. S.; Peng, H.; Ringe, S.; Hahn, C.; Jaramillo, T. F.; Nørskov, J. K.; Chan, K., pH effects on the electrochemical reduction of CO₍₂₎ towards C₂ products on stepped copper. *Nat. Commun.* **2019**, *10* (1), 32.

- 14. Dunwell, M.; Yang, X.; Setzler, B. P.; Anibal, J.; Yan, Y.; Xu, B., Examination of near-electrode concentration gradients and kinetic impacts on the electrochemical reduction of CO₂ using surface-enhanced infrared spectroscopy. *ACS Catal.* **2018**, *8* (5), 3999-4008.
- 15. Hall, A. S.; Yoon, Y.; Wuttig, A.; Surendranath, Y., Mesostructure-induced selectivity in CO₂ reduction catalysis. *J. Am. Chem. Soc.* **2015**, *137* (47), 14834-14837.
- 16. Xiao, H.; Cheng, T.; Goddard, W. A.; Sundararaman, R., Mechanistic explanation of the pH dependence and onset potentials for hydrocarbon products from electrochemical reduction of CO on Cu (111). *J. Am. Chem. Soc.* **2016**, *138* (2), 483-486.
- 17. Dinh, C.-T.; Burdyny, T.; Kibria, M. G.; Seifitokaldani, A.; Gabardo, C. M.; García de Arquer, F. P.; Kiani, A.; Edwards, J. P.; De Luna, P.; Bushuyev, O. S.; Zou, C.; Quintero-Bermudez, R.; Pang, Y.; Sinton, D.; Sargent, E. H., CO₂ electroreduction to ethylene via hydroxide-mediated copper catalysis at an abrupt interface. *Science* **2018**, *360* (6390), 783.
- 18. Kim, B.; Ma, S.; Molly Jhong, H.-R.; Kenis, P. J. A., Influence of dilute feed and pH on electrochemical reduction of CO₂ to CO on Ag in a continuous flow electrolyzer. *Electrochim*. *Acta* **2015**, *166*, 271-276.
- 19. Gao, D. F.; Wang, J.; Wu, H. H.; Jiang, X. L.; Miao, S.; Wang, G. X.; Bao, X. H., pH effect on electrocatalytic reduction of CO₂ over Pd and Pt nanoparticles. *Electrochem. Commun.* **2015**, *55*, 1-5.
- 20. Kas, R.; Kortlever, R.; Yılmaz, H.; Koper, M. T. M.; Mul, G., Manipulating the hydrocarbon selectivity of copper nanoparticles in CO₂ electroreduction by process conditions. *ChemElectroChem* **2015**, *2* (3), 354-358.

- 21. Resasco, J.; Lum, Y.; Clark, E.; Zeledon, J. Z.; Bell, A. T., Effects of anion identity and concentration on electrochemical reduction of CO₂. *ChemElectroChem* **2018**, *5* (7), 1064-1072.
- 22. Verma, S.; Lu, X.; Ma, S.; Masel, R. I.; Kenis, P. J. A., The effect of electrolyte composition on the electroreduction of CO₂ to CO on Ag based gas diffusion electrodes. *Phys. Chem. Chem. Phys.* **2016**, *18* (10), 7075-7084.
- 23. Moura de Salles Pupo, M.; Kortlever, R., Electrolyte effects on the electrochemical reduction of CO₂. *ChemPhysChem* **2019**, *20*, 2926-2935.
- 24. Thorson, M. R.; Siil, K. I.; Kenis, P. J. A., Effect of cations on the electrochemical conversion of CO₂ to CO. *J. Electrochem. Soc.* **2013**, *160* (1), F69-F74.
- 25. Matsubara, Y.; Grills, D. C.; Kuwahara, Y., Thermodynamic aspects of electrocatalytic CO₂ reduction in acetonitrile and with an ionic liquid as solvent or electrolyte. *ACS Catal.* **2015**, *5* (11), 6440-6452.
- 26. Murugananthan, M.; Kumaravel, M.; Katsumata, H.; Suzuki, T.; Kaneco, S., Electrochemical reduction of CO₂ using Cu electrode in methanol/LiClO₄ electrolyte. *Int. J. Hydrogen Energy* **2015**, *40* (21), 6740-6744.
- 27. Kaneco, S.; Katsumata, H.; Suzuki, T.; Ohta, K., Electrochemical reduction of CO₂ to methane at the Cu electrode in methanol with sodium supporting salts and its comparison with other alkaline salts. *Energy Fuels* **2006**, *20* (1), 409-414.

- 28. Rosen, B. A.; Salehi-Khojin, A.; Thorson, M. R.; Zhu, W.; Whipple, D. T.; Kenis, P. J. A.; Masel, R. I., Ionic liquid-mediated selective conversion of CO₂ to CO at low overpotentials. *Science* **2011**, *334* (6056), 643-644.
- 29. Tanner, E. E. L.; Batchelor-McAuley, C.; Compton, R. G., Carbon dioxide reduction in room-temperature ionic liquids: The effect of the choice of electrode material, cation, and anion. *J. Phys. Chem. C* **2016**, *120* (46), 26442-26447.
- 30. Atifi, A.; Boyce, D. W.; DiMeglio, J. L.; Rosenthal, J., Directing the outcome of CO₂ reduction at bismuth cathodes using varied ionic liquid promoters. *ACS Catal.* **2018**, *8* (4), 2857-2863.
- 31. Gattrell, M.; Gupta, N.; Co, A., A review of the aqueous electrochemical reduction of CO₂ to hydrocarbons at copper. *J. Electroanal. Chem.* **2006**, *594* (1), 1-19.
- 32. Weng, Z.; Jiang, J.; Wu, Y.; Wu, Z.; Guo, X.; Materna, K. L.; Liu, W.; Batista, V. S.; Brudvig, G. W.; Wang, H., Electrochemical CO₂ reduction to hydrocarbons on a heterogeneous molecular Cu catalyst in aqueous solution. *J. Am. Chem. Soc.* **2016**, *138* (26), 8076-8079.
- 33. Quan, F.; Xiong, M.; Jia, F.; Zhang, L., Efficient electroreduction of CO₂ on bulk silver electrode in aqueous solution via the inhibition of hydrogen evolution. *Appl. Surf. Sci.* **2017**, *399*, 48-54.
- 34. Liu, M.; Pang, Y.; Zhang, B.; De Luna, P.; Voznyy, O.; Xu, J.; Zheng, X.; Dinh, C. T.; Fan, F.; Cao, C.; de Arquer, F. P. G.; Safaei, T. S.; Mepham, A.; Klinkova, A.; Kumacheva, E.; Filleter, T.; Sinton, D.; Kelley, S. O.; Sargent, E. H., Enhanced electrocatalytic CO₂ reduction via field-induced reagent concentration. *Nature* **2016**, *537* (7620), 382-386.

- 35. Zhong, H.; Fujii, K.; Nakano, Y., Effect of KHCO₃ concentration on electrochemical reduction of CO₂ on copper electrode. *J. Electrochem. Soc.* **2017**, *164* (9), F923-F927.
- 36. Murata, A.; Hori, Y., Product selectivity affected by cationic species in electrochemical reduction of CO₂ and CO at a Cu electrode. *Bull. Chem. Soc. Jpn.* **1991,** *64* (1), 123-127.
- 37. Hori, Y.; Suzuki, S., Electrolytic reduction of carbon-dioxide at mercury-electrode in aqueous-solution. *Bull. Chem. Soc. Jpn.* **1982**, *55* (3), 660-665.
- 38. Wu, J. J.; Risalvato, F. G.; Ke, F. S.; Pellechia, P. J.; Zhou, X. D., Electrochemical reduction of carbon dioxide I. Effects of the electrolyte on the selectivity and activity with Sn electrode. *J. Electrochem. Soc.* **2012**, *159* (7), F353-F359.
- 39. Yano, H.; Tanaka, T.; Nakayama, M.; Ogura, K., Selective electrochemical reduction of CO₂ to ethylene at a three-phase interface on copper(I) halide-confined Cu-mesh electrodes in acidic solutions of potassium halides. *J. Electroanal. Chem.* **2004**, *565* (2), 287-293.
- 40. Zhou, F.; Liu, S.; Yang, B.; Wang, P.; Alshammari, A. S.; Deng, Y., Highly selective electrocatalytic reduction of carbon dioxide to carbon monoxide on silver electrode with aqueous ionic liquids. *Electrochem. Commun.* **2014**, *46*, 103-106.
- 41. Sharifi Golru, S.; Biddinger, E. J., Effect of anion in diluted imidazolium-based ionic liquid/buffer electrolytes for CO₂ electroreduction on copper. *Electrochim. Acta* **2020**, *375*, 136787.
- 42. Feaster, J. T.; Jongerius, A. L.; Liu, X. Y.; Urushihara, M.; Nitopi, S. A.; Hahn, C.; Chan, K.; Norskov, J. K.; Jaramillo, T. F., Understanding the influence of EMIM CI on the

suppression of the hydrogen evolution reaction on transition metal electrodes. *Langmuir* **2017**, *33* (37), 9464-9471.

- 43. Hailu, A.; Shaw, S. K., Efficient electrocatalytic reduction of carbon dioxide in 1-ethyl-3-methylimidazolium trifluoromethanesulfonate and water mixtures. *Energy Fuels* **2018**, *32* (12), 12695-12702.
- 44. Zarandi, R. F.; Rezaei, B.; Ghaziaskar, H. S.; Ensafi, A. A., Electrochemical reduction of CO₂ to ethanol using copper nanofoam electrode and 1-butyl-3-methyl-imidazolium bromide as the homogeneous co-catalyst. *J. Environ. Chem. Eng.* **2019**, *7* (3), 103141.
- 45. Rudnev, A. V.; Kiran, K.; Cedeño López, A.; Dutta, A.; Gjuroski, I.; Furrer, J.; Broekmann, P., Enhanced electrocatalytic CO formation from CO₂ on nanostructured silver foam electrodes in ionic liquid/water mixtures. *Electrochim. Acta* **2019**, *306*, 245-253.
- 46. Huan, T. N.; Simon, P.; Rousse, G.; Génois, I.; Artero, V.; Fontecave, M., Porous dendritic copper: an electrocatalyst for highly selective CO₂ reduction to formate in water/ionic liquid electrolyte. *Chem. Sci.* **2017**, *8* (1), 742-747.
- 47. Han, Z.; Kortlever, R.; Chen, H.-Y.; Peters, J. C.; Agapie, T., CO₂ reduction selective for C≥2 products on polycrystalline copper with N-substituted pyridinium additives. *ACS Cent. Sci.* **2017**, *3* (8), 853-859.
- 48. Dufek, E. J.; Lister, T. E.; McIlwain, M. E., Influence of electrolytes and membranes on cell operation for syn-gas production. *Electrochem. Solid-State Lett.* **2012**, *15* (4), B48.

- 49. Lv, J.-J.; Jouny, M.; Luc, W.; Zhu, W.; Zhu, J.-J.; Jiao, F., A highly porous copper electrocatalyst for carbon dioxide reduction. *Adv. Mater.* **2018**, *30* (49), 1803111.
- 50. Thevenon, A.; Rosas-Hernández, A.; Peters, J. C.; Agapie, T., In-situ nanostructuring and stabilization of polycrystalline copper by an organic salt additive promotes electrocatalytic CO₂ reduction to ethylene. *Angew. Chem., Int. Ed.* **2019**, *58* (47), 16952-16958.
- 51. Banerjee, S.; Han, X.; Thoi, V. S., Modulating the electrode-electrolyte interface with cationic surfactants in carbon dioxide reduction. *ACS Catal.* **2019**, *9* (6), 5631-5637.
- 52. Huang, Y.; Ong, C. W.; Yeo, B. S., Effects of electrolyte anions on the reduction of carbon dioxide to ethylene and ethanol on copper (100) and (111) surfaces. *Chemsuschem* **2018**, *11* (18), 3299-3306.
- 53. Gao, D. F.; Sohoken, F.; Roldan Cuenya, B., Improved CO₂ electroreduction performance on plasma-activated Cu catalysts via electrolyte design: Halide effect. *ACS Catal.* **2017,** 7 (8), 5112-5120.
- 54. Varela, A. S.; Ju, W.; Reier, T.; Strasser, P., Tuning the catalytic activity and selectivity of Cu for CO₂ electroreduction in the presence of halides. *ACS Catal.* **2016**, *6* (4), 2136-2144.
- 55. Salehi-Khojin, A.; Jhong, H.-R. M.; Rosen, B. A.; Zhu, W.; Ma, S.; Kenis, P. J. A.; Masel, R. I., Nanoparticle silver catalysts that Show enhanced activity for carbon dioxide electrolysis. *J. Phys. Chem. C* **2013**, *117* (4), 1627-1632.

- 56. Rudnev, A. V.; Fu, Y. C.; Gjuroski, I.; Stricker, F.; Furrer, J.; Kovacs, N.; Vesztergom, S.; Broekmann, P., Transport matters: Boosting CO₂ electroreduction in mixtures of BMIm BF₄/water by enhanced diffusion. *Chemphyschem* **2017**, *18* (22), 3153-3162.
- 57. Zhang, X.; Zhao, Y.; Hu, S.; Gliege, M. E.; Liu, Y.; Liu, R.; Scudiero, L.; Hu, Y.; Ha, S., Electrochemical reduction of carbon dioxide to formic acid in ionic liquid [Emim][N(CN)₂]/water system. *Electrochim. Acta* **2017**, *247*, 281-287.
- 58. Dong, Q.; Zhang, X. Z.; He, D.; Lang, C. C.; Wang, D. W., Role of H₂O in CO₂ electrochemical reduction as studied in a water-in-salt system. *ACS Cent. Sci.* **2019**, *5* (8), 1461-1467.
- 59. Hong, S.; Lee, S.; Kim, S.; Lee, J. K.; Lee, J., Anion dependent CO/H₂ production ratio from CO₂ reduction on Au electro-catalyst. *Catal. Today* **2017**, *295*, 82-88.
- 60. Neubauer, S. S.; Krause, R. K.; Schmid, B.; Guldi, D. M.; Schmid, G., Overpotentials and faraday efficiencies in CO₂ electrocatalysis—the impact of 1-ethyl-3-methylimidazolium trifluoromethanesulfonate. *Adv. Energy Mater.* **2016**, *6* (9), 1502231.
- 61. Hanc-Scherer, F. A.; Montiel, M. A.; Montiel, V.; Herrero, E.; Sánchez-Sánchez, C. M., Surface structured platinum electrodes for the electrochemical reduction of carbon dioxide in imidazolium based ionic liquids. *Phys. Chem. Chem. Phys.* **2015**, *17* (37), 23909-23916.
- 62. Jones, J. P.; Prakash, G. K. S.; Olah, G. A., Electrochemical CO₂ reduction: Recent advances and current trends. *Isr. J. Chem.* **2014**, *54* (10), 1451-1466.

- 63. Qiao, J.; Liu, Y.; Hong, F.; Zhang, J., A review of catalysts for the electroreduction of carbon dioxide to produce low-carbon fuels. *Chem. Soc. Rev.* **2014**, *43* (2), 631-675.
- 64. Long, C.; Li, X.; Guo, J.; Shi, Y.; Liu, S.; Tang, Z., Electrochemical reduction of CO₂ over heterogeneous catalysts in aqueous solution: Recent progress and perspectives. *Small Methods* **2019**, *3* (3), 1800369.
- 65. Lu, Q.; Jiao, F., Electrochemical CO₂ reduction: Electrocatalyst, reaction mechanism, and process engineering. *Nano Energy* **2016**, *29*, 439-456.
- 66. Ma, S. C.; Lan, Y. C.; Perez, G. M. J.; Moniri, S.; Kenis, P. J. A., Silver supported on titania as an active catalyst for electrochemical carbon dioxide reduction. *Chemsuschem* **2014**, *7* (3), 866-874.
- 67. Leonard, M. E.; Clarke, L. E.; Forner-Cuenca, A.; Brown, S. M.; Brushett, F. R., Investigating electrode flooding in a flowing electrolyte, gas-fed carbon dioxide electrolyzer. *Chemsuschem* **2020**, *13* (2), 400-411.
- 68. Verma, S.; Hamasaki, Y.; Kim, C.; Huang, W. X.; Lu, S.; Jhong, H. R. M.; Gewirth, A. A.; Fujigaya, T.; Nakashima, N.; Kenis, P. J. A., Insights into the low overpotential electroreduction of CO₂ to CO on a supported gold catalyst in an alkaline flow electrolyzer. *ACS Energy Lett.* **2018**, *3* (1), 193-198.
- 69. Larrazabal, G. O.; Strom-Hansen, P.; Heli, J. P.; Zeiter, K.; Therldldsen, K. T.; Chorkendorff, I.; Seger, B., Analysis of mass flows and membrane cross-over in CO₂ reduction at high current densities in an MEA-type electrolyzer. *ACS Appl. Mater. Interfaces* **2019**, *11* (44), 41281-41288.

- 70. Zhang, J.; Luo, W.; Zuttel, A., Crossover of liquid products from electrochemical CO₂ reduction through gas diffusion electrode and anion exchange membrane. *J. Catal.* **2020**, *385*, 140-145.
- 71. Chen, L. D.; Urushihara, M.; Chan, K.; Nørskov, J. K., Electric field effects in electrochemical CO₂ reduction. *ACS Catal.* **2016**, *6* (10), 7133-7139.
- 72. Akhade, S. A.; McCrum, I. T.; Janik, M. J., The impact of specifically adsorbed ions on the copper-catalyzed electroreduction of CO₂. *J. Electrochem. Soc.* **2016**, *163* (6), F477-F484.
- 73. Banerjee, S.; Zhang, Z. Q.; Hall, A. S.; Thoi, V. S., Surfactant perturbation of cation interactions at the electrode-electrolyte interface in carbon dioxide reduction. *ACS Catal.* **2020**, *10* (17), 9907-9914.
- 74. Hori, Y.; Murata, A.; Takahashi, R., Formation of hydrocarbons in the electrochemical reduction of carbon dioxide at a copper electrode in aqueous solution. *J. Chem. Soc., Faraday Trans. 1* **1989**, *85* (8), 2309-2326.
- 75. Hori, Y.; Wakebe, H.; Tsukamoto, T.; Koga, O., Electrocatalytic process of CO selectivity in electrochemical reduction of CO₂ at metal electrodes in aqueous media. *Electrochim. Acta* **1994**, *39* (11–12), 1833-1839.
- 76. Hori, Y.; Murata, A.; Takahashi, R.; Suzuki, S., Enhanced formation of ethylene and alcohols at ambient temperature and pressure in electrochemical reduction of carbon dioxide at a copper electrode. *J. Chem. Soc., Chem. Commun.* **1988,** (1), 17-19.

- 77. Varela, A. S.; Kroschel, M.; Reier, T.; Strasser, P., Controlling the selectivity of CO₂ electroreduction on copper: The effect of the electrolyte concentration and the importance of the local pH. *Catal. Today* **2016**, *260*, 8-13.
- 78. Chen, C. S.; Handoko, A. D.; Wan, J. H.; Ma, L.; Ren, D.; Yeo, B. S., Stable and selective electrochemical reduction of carbon dioxide to ethylene on copper mesocrystals. *Catal. Sci. Technol.* **2015**, *5* (1), 161-168.
- 79. Roberts, F. S.; Kuhl, K. P.; Nilsson, A., High selectivity for ethylene from carbon dioxide reduction over copper nanocube electrocatalysts. *Angew. Chem., Int. Ed.* **2015,** *54* (17), 5179-5182.
- 80. Kwon, Y.; Lum, Y.; Clark, E. L.; Ager, J. W.; Bell, A. T., CO₂ electroreduction with enhanced ethylene and ethanol selectivity by nanostructuring polycrystalline copper.

 ChemElectroChem 2016, 3 (6), 1012-1019.
- 81. Ovalle, V. J.; Waegele, M. M., Impact of electrolyte anions on the adsorption of CO on Cu electrodes. *J. Phys. Chem. C* **2020**, *124* (27), 14713-14721.
- 82. Wuttig, A.; Yaguchi, M.; Motobayashi, K.; Osawa, M.; Surendranath, Y., Inhibited proton transfer enhances Au-catalyzed CO₂-to-fuels selectivity. *Proc. Natl. Acad. Sci. U. S. A.* **2016**, *113* (32), E4585-E4593.
- 83. Dunwell, M.; Lu, Q.; Heyes, J. M.; Rosen, J.; Chen, J. G. G.; Yan, Y. S.; Jiao, F.; Xu, B. J., The central role of bicarbonate in the electrochemical reduction of carbon dioxide on gold. *J. Am. Chem. Soc.* **2017**, *139* (10), 3774-3783.

- 84. Zhu, S. Q.; Jiang, B.; Cai, W. B.; Shao, M. H., Direct observation on reaction intermediates and the role of bicarbonate anions in CO₂ electrochemical reduction reaction on Cu surfaces. *J. Am. Chem. Soc.* **2017**, *139* (44), 15664-15667.
- 85. Ogura, K.; Ferrell, J. R.; Cugini, A. V.; Smotkin, E. S.; Salazar-Villalpando, M. D., CO₂ attraction by specifically adsorbed anions and subsequent accelerated electrochemical reduction. *Electrochim. Acta* **2010**, *56* (1), 381-386.
- 86. Singh, M. R.; Kwon, Y.; Lum, Y.; Ager, J. W.; Bell, A. T., Hydrolysis of electrolyte cations enhances the electrochemical reduction of CO₂ over Ag and Cu. *J. Am. Chem. Soc.* **2016**, *138* (39), 13006-13012.
- 87. Resasco, J.; Chen, L. D.; Clark, E.; Tsai, C.; Hahn, C.; Jaramillo, T. F.; Chan, K.; Bell, A. T., Promoter effects of alkali metal cations on the electrochemical reduction of carbon dioxide. *J. Am. Chem. Soc.* **2017**, *139* (32), 11277-11287.
- 88. Asadi, M.; Kumar, B.; Behranginia, A.; Rosen, B. A.; Baskin, A.; Repnin, N.; Pisasale, D.; Phillips, P.; Zhu, W.; Haasch, R.; Klie, R. F.; Král, P.; Abiade, J.; Salehi-Khojin, A., Robust carbon dioxide reduction on molybdenum disulphide edges. *Nat. Commun.* **2014**, *5*, 4470.
- 89. Gunathunge, C. M.; Ovalle, V. J.; Waegele, M. M., Probing promoting effects of alkali cations on the reduction of CO at the aqueous electrolyte/copper interface. *Phys. Chem. Chem. Phys.* **2017**, *19* (44), 30166-30172.

- 90. Li, J. Y.; Li, X.; Gunathunge, C. M.; Waegele, M. M., Hydrogen bonding steers the product selectivity of electrocatalytic CO reduction. *Proc. Natl. Acad. Sci. U. S. A.* **2019**, *116* (19), 9220-9229.
- 91. Malkani, A. S.; Anibal, J.; Xu, B., Cation effect on interfacial CO₂ concentration in the electrochemical CO₂ reduction reaction. *ACS Catal.* **2020**, *10* (24), 14871-14876.
- 92. Ogura, K., Electrochemical reduction of carbon dioxide to ethylene: Mechanistic approach. *J. CO2 Util.* **2013**, *1*, 43-49.
- 93. Asadi, M.; Kim, K.; Liu, C.; Addepalli, A. V.; Abbasi, P.; Yasaei, P.; Phillips, P.; Behranginia, A.; Cerrato, J. M.; Haasch, R.; Zapol, P.; Kumar, B.; Klie, R. F.; Abiade, J.; Curtiss, L. A.; Salehi-Khojin, A., Nanostructured transition metal dichalcogenide electrocatalysts for CO₂ reduction in ionic liquid. *Science* **2016**, *353* (6298), 467.
- 94. Kyriacou, G. Z.; Anagnostopoulos, A. K., Influence of CO₂ partial-pressure and the supporting electrolyte cation on the product distribution in CO₂ electroreduction. *J. Appl. Electrochem.* **1993**, *23* (5), 483-486.
- 95. Hsieh, Y. C.; Senanayake, S. D.; Zhang, Y.; Xu, W. Q.; Polyansky, D. E., Effect of chloride anions on the synthesis and enhanced catalytic activity of silver nanocoral electrodes for CO₂ electroreduction. *ACS Catal.* **2015**, *5* (9), 5349-5356.
- 96. Huang, J. C.; O'Grady, W. E.; Yeager, E., The effects of cations and anions on hydrogen chemisorption at Pt. *J. Electrochem. Soc.* **1977**, *124* (11), 1732-1737.

- 97. Hsieh, Y. C.; Betancourt, L. E.; Senanayake, S. D.; Hu, E. Y.; Zhang, Y.; Xu, W. Q.; Polyansky, D. E., Modification of CO₂ reduction activity of nanostructured silver electrocatalysts by surface halide anions. *ACS Appl. Energy Mater.* **2019**, *2* (1), 102-109.
- 98. Cho, M.; Song, J. T.; Back, S.; Jung, Y.; Oh, J., The role of adsorbed CN and Cl on an Au electrode for electrochemical CO₂ reduction. *ACS Catal.* **2018**, 8 (2), 1178-1185.
- 99. Varela, A. S., The importance of pH in controlling the selectivity of the electrochemical CO₂ reduction. *Curr. Opin. Green Sustain. Chem.* **2020**, *26*.
- 100. Kortlever, R.; Shen, J.; Schouten, K. J. P.; Calle-Vallejo, F.; Koper, M. T. M., Catalysts and reaction pathways for the electrochemical reduction of carbon dioxide. *J. Phys. Chem. Lett.* **2015,** *6* (20), 4073-4082.
- 101. Tripkovic, D. V.; Strmcnik, D.; van der Vliet, D.; Stamenkovic, V.; Markovic, N. M., The role of anions in surface electrochemistry. *Faraday Discuss.* **2008**, *140*, 25-40.
- 102. McCrum, I. T.; Akhade, S. A.; Janik, M. J., Electrochemical specific adsorption of halides on Cu 111,100, and 211: A Density Functional Theory study. *Electrochim. Acta* **2015**, *173*, 302-309.
- 103. Montoya, J. H.; Shi, C.; Chan, K.; Nørskov, J. K., Theoretical insights into a CO dimerization mechanism in CO₂ electroreduction. *J. Phys. Chem. Lett.* **2015**, *6* (11), 2032-2037.
- 104. Shaw, S. K.; Berna, A.; Feliu, J. M.; Nichols, R. J.; Jacob, T.; Schiffrin, D. J., Role of axially coordinated surface sites for electrochemically controlled carbon monoxide adsorption on single crystal copper electrodes. *Phys. Chem. Chem. Phys.* **2011**, *13* (12), 5242-5251.

- 105. Blyholder, G., Molecular orbital view of chemisorbed carbon monoxide. *J. Phys. Chem.* **1964,** *68* (10), 2772-&.
- 106. Ogura, K.; Salazar-Villalpando, M. D., CO₂ electrochemical reduction via adsorbed halide anions. *Jom* **2011**, *63* (1), 35-38.
- 107. Kortlever, R.; Tan, K. H.; Kwon, Y.; Koper, M. T. M., Electrochemical carbon dioxide and bicarbonate reduction on copper in weakly alkaline media. *J. Solid State Electrochem.* **2013**, *17* (7), 1843-1849.
- 108. Freund, H. J.; Roberts, M. W., Surface chemistry of carbon dioxide. *Surf. Sci. Rep.* **1996**, 25 (8), 225-273.
- 109. Bockris, J. O. M.; Conway, B. E.; Yeager, E., *Comprehensive treatise of electrochemistry: Vol.1: The double layer.* Plenum Press: 1980.
- 110. Kamalakannan, S.; Prakash, M.; Chambaud, G.; Hochlaf, M., Adsorption of hydrophobic and hydrophilic ionic liquids at the Au(111) surface. *ACS Omega* **2018**, *3* (12), 18039-18051.
- 111. Schizodimou, A.; Kyriacou, G., Acceleration of the reduction of carbon dioxide in the presence of multivalent cations. *Electrochim. Acta* **2012,** *78*, 171-176.
- 112. Ferapontova, E. E.; Fedorovich, N. V., Effect of cation adsorption on the kinetics of anion electroreduction Part I. Effect of the adsorption of inorganic cations in small concentrations on the kinetics of anion electroreduction with different elementary steps of discharge. *J. Electroanal. Chem.* **1999**, *476* (1), 26-36.

- 113. Damaskin, B. B.; Safonov, V. A.; Fedorovich, N. V., Some specific features of the effect of multicharged cations on the electroreduction of anions. *J. Electroanal. Chem.* **1993**, *349* (1-2), 1-14.
- 114. Lukomska, A.; Sobkowski, J., Potential of zero charge of monocrystalline copper electrodes in perchlorate solutions. *J. Electroanal. Chem.* **2004**, *567* (1), 95-102.
- 115. Strmcnik, D.; Kodama, K.; van der Vliet, D.; Greeley, J.; Stamenkovic, V. R.; Markovic, N. M., The role of non-covalent interactions in electrocatalytic fuel-cell reactions on platinum. *Nat. Chem.* **2009**, *1* (6), 466-472.
- 116. Ayemoba, O.; Cuesta, A., Spectroscopic evidence of size-dependent buffering of interfacial pH by cation hydrolysis during CO₂ electroreduction. *ACS Appl. Mater. Interfaces* **2017**, *9* (33), 27377-27382.
- 117. Ringe, S.; Clark, E. L.; Resasco, J.; Walton, A.; Seger, B.; Bell, A. T.; Chan, K., Understanding cation effects in electrochemical CO₂ reduction. *Energy Environ. Sci.* **2019**, *12* (10), 3001-3014.
- 118. Sandberg, R. B.; Montoya, J. H.; Chan, K.; Norskov, J. K., CO-CO coupling on Cu facets: Coverage, strain and field effects. *Surf. Sci.* **2016**, *654*, 56-62.
- 119. Kaneco, S.; Katsumata, H.; Suzuki, T.; Ohta, K., Electrochemical reduction of carbon dioxide to ethylene at a copper electrode in methanol using potassium hydroxide and rubidium hydroxide supporting electrolytes. *Electrochim. Acta* **2006**, *51* (16), 3316-3321.

- 120. Spichigerulmann, M.; Augustynski, J., Remarkable enhancement of the rate of cathodic reduction of hydrocarbonate anions at palladium in the presence of cesium cations. *Helv. Chim. Acta* **1986**, *69* (3), 632-634.
- 121. Papasizza, M.; Cuesta, A., In situ monitoring using ATR-SEIRAS of the electrocatalytic reduction of CO₂ on Au in an ionic liquid/water mixture. *ACS Catal.* **2018**, 8 (7), 6345-6352.
- 122. Gao, D. F.; McCrum, I. T.; Deo, S.; Choi, Y. W.; Scholten, F.; Wan, W. M.; Chen, J. G. G.; Janik, M. J.; Roldan Cuenya, B., Activity and selectivity control in CO₂ electroreduction to multicarbon products over CuO_x catalysts via electrolyte design. *ACS Catal.* **2018**, *8* (11), 10012-+.
- 123. Wu, H.; Song, J.; Xie, C.; Hu, Y.; Han, B., Highly efficient electrochemical reduction of CO₂ into formic acid over lead dioxide in an ionic liquid–catholyte mixture. *Green Chem.*2018, 20 (8), 1765-1769.
- 124. Hasib-ur-Rahman, M.; Siaj, M.; Larachi, F., Ionic liquids for CO₂ capture-Development and progress. *Chem. Eng. Process.* **2010**, *49* (4), 313-322.
- 125. Abdinejad, M.; Mirza, Z.; Zhang, X.-a.; Kraatz, H.-B., Enhanced electrocatalytic activity of primary amines for CO₂ reduction using copper electrodes in aqueous solution. *ACS Sustainable Chem. Eng.* **2020**.
- 126. Morris, A. J.; McGibbon, R. T.; Bocarsly, A. B., Electrocatalytic carbon dioxide activation: The rate-determining step of pyridinium-catalyzed CO₂ reduction. *ChemSusChem* **2011**, *4* (2), 191-196.

- 127. Barton Cole, E.; Lakkaraju, P. S.; Rampulla, D. M.; Morris, A. J.; Abelev, E.; Bocarsly, A. B., Using a one-electron shuttle for the multielectron reduction of CO₂ to methanol: kinetic, mechanistic, and structural insights. *J. Am. Chem. Soc.* **2010**, *132* (33), 11539-11551.
- 128. Albo, J.; Beobide, G.; Castano, P.; Irabien, A., Methanol electrosynthesis from CO₂ at Cu₂O/ZnO prompted by pyridine-based aqueous solutions. *J. CO2 Util.* **2017**, *18*, 164-172.
- 129. Bocarsly, A. B.; Gibson, Q. D.; Morris, A. J.; L'Esperance, R. P.; Detweiler, Z. M.; Lakkaraju, P. S.; Zeitler, E. L.; Shaw, T. W., Comparative study of imidazole and pyridine catalyzed reduction of carbon dioxide at illuminated iron pyrite electrodes. *ACS Catal.* **2012**, *2* (8), 1684-1692.
- 130. Zanchet, L.; da Trindade, L. G.; Lima, D. W.; Bariviera, W.; Trombetta, F.; de Souza, M. O.; Martini, E. M. A., Cation influence of new imidazolium-based ionic liquids on hydrogen production from water electrolysis. *Ionics* **2019**, *25* (3), 1167-1176.
- 131. Waluyo, I.; Huang, C. C.; Nordlund, D.; Bergmann, U.; Weiss, T. M.; Pettersson, L. G. M.; Nilsson, A., The structure of water in the hydration shell of cations from x-ray Raman and small angle x-ray scattering measurements. *J. Chem. Phys.* **2011**, *134* (6).
- 132. Rosen, B. A.; Haan, J. L.; Mukherjee, P.; Braunschweig, B.; Zhu, W.; Salehi-Khojin, A.; Dlott, D. D.; Masel, R. I., In situ spectroscopic examination of a low overpotential pathway for carbon dioxide conversion to carbon monoxide. *J. Phys. Chem. C* **2012**, *116* (29), 15307-15312.
- 133. Sun, L.; Ramesha, G. K.; Kamat, P. V.; Brennecke, J. F., Switching the reaction course of electrochemical CO₂ reduction with ionic liquids. *Langmuir* **2014**, *30* (21), 6302-6308.

- 134. Niu, D.; Wang, H.; Li, H.; Wu, Z.; Zhang, X., Roles of ion pairing on electroreduction of carbon dioxide based on imidazolium-based salts. *Electrochim. Acta* **2015**, *158*, 138-142.
- 135. Kemna, A.; Rey, N. G.; Braunschweig, B., Mechanistic insights on CO₂ reduction reactions at platinum/ BMIM BF₄ interfaces from in operando spectroscopy. *ACS Catal.* **2019**, *9* (7), 6284-6292.
- 136. Wang, Y. Q.; Hatakeyama, M.; Ogata, K.; Wakabayashi, M.; Jin, F. M.; Nakamura, S., Activation of CO₂ by ionic liquid EMIM-BF₄ in the electrochemical system: a theoretical study. *Phys. Chem. Chem. Phys.* **2015**, *17* (36), 23521-23531.
- 137. Lau, G. P. S.; Schreier, M.; Vasilyev, D.; Scopelliti, R.; Grätzel, M.; Dyson, P. J., New insights into the role of imidazolium-based promoters for the electroreduction of CO₂ on a silver electrode. *J. Am. Chem. Soc.* **2016**, *138* (25), 7820-7823.
- 138. Urushihara, M.; Chan, K.; Shi, C.; Nørskov, J. K., Theoretical study of EMIM⁺ adsorption on silver electrode surfaces. *J. Phys. Chem. C* **2015**, *119* (34), 20023-20029.
- 139. Wang, Y.; Hayashi, T.; He, D. P.; Li, Y. M.; Jin, F. M.; Nakamura, R., A reduced imidazolium cation layer serves as the active site for electrochemical carbon dioxide reduction. *Appl. Catal.*, B **2020**, *264*.
- 140. Zhao, S. F.; Horne, M.; Bond, A. M.; Zhang, J., Is the imidazolium cation a unique promoter for electrocatalytic reduction of carbon dioxide? *J. Phys. Chem. C* **2016**, *120* (42), 23989-24001.

- 141. Lim, H.-K.; Kwon, Y.; Kim, H. S.; Jeon, J.; Kim, Y.-H.; Lim, J.-A.; Kim, B.-S.; Choi, J.; Kim, H., Insight into the microenvironments of the metal–ionic liquid interface during electrochemical CO₂ reduction. *ACS Catal.* **2018**, *8* (3), 2420-2427.
- 142. Gebbie, M. A.; Valtiner, M.; Banquy, X.; Fox, E. T.; Henderson, W. A.; Israelachvili, J. N., Ionic liquids behave as dilute electrolyte solutions. *Proc. Natl. Acad. Sci. U. S. A.* **2013,** *110* (24), 9674-9679.
- 143. Nanbu, N.; Sasaki, Y.; Kitamura, F., In situ FT-IR spectroscopic observation of a room-temperature molten salt vertical bar gold electrode interphase. *Electrochem. Commun.* **2003**, *5* (5), 383-387.
- 144. Yuan, Y. X.; Niu, T. C.; Xu, M. M.; Yao, J. L.; Gu, R. A., Probing the adsorption of methylimidazole at ionic liquids/Cu electrode interface by surface-enhanced Raman scattering spectroscopy. *J. Raman Spectrosc.* **2010**, *41* (5), 516-523.
- 145. Baldelli, S., Surface structure at the ionic liquid-electrified metal interface. *Acc. Chem. Res.* **2008**, *41* (3), 421-431.
- 146. Lockett, V.; Sedev, R.; Ralston, J.; Horne, M.; Rodopoulos, T., Differential capacitance of the electrical double layer in imidazolium-based ionic liquids: Influence of potential, cation size, and temperature. *J. Phys. Chem. C* **2008**, *112* (19), 7486-7495.
- 147. Feng, G.; Jiang, X. K.; Qiao, R.; Kornyshev, A. A., Water in ionic liquids at electrified interfaces: The anatomy of electrosorption. *ACS Nano* **2014**, *8* (11), 11685-11694.

- 148. Rosen, B. A.; Zhu, W.; Kaul, G.; Salehi-Khojin, A.; Masel, R. I., Water enhancement of CO₂ conversion on silver in 1-ethyl-3-methylimidazolium tetrafluoroborate. *J. Electrochem. Soc.* **2013**, *160* (2), H138-H141.
- 149. Motobayashi, K.; Osawa, M., Potential-dependent condensation of water at the interface between ionic liquid [BMIM][TFSA] and an Au electrode. *Electrochem. Commun.* **2016,** *65*, 14-17.
- 150. Osawa, M.; Tsushima, M.; Mogami, H.; Samjeske, G.; Yamakata, A., Structure of water at the electrified platinum-water interface: A study by surface-enhanced infrared absorption spectroscopy. *J. Phys. Chem. C* **2008**, *112* (11), 4248-4256.
- 151. Ataka, K.; Yotsuyanagi, T.; Osawa, M., Potential-dependent reorientation of water molecules at an electrode/electrolyte interface studied by surface-enhanced infrared absorption spectroscopy. *J. Phys. Chem.* **1996**, *100* (25), 10664-10672.
- 152. Zhang, Z. Q.; Banerjee, S.; Thoi, V. S.; Hall, A. S., Reorganization of interfacial water by an amphiphilic cationic surfactant promotes CO₂ reduction. *J. Phys. Chem. Lett.* **2020**, *11* (14), 5457-5463.
- 153. Santos, V. O.; Alves, M. B.; Carvalho, M. S.; Suarez, P. A. Z.; Rubim, J. C., Surface-enhanced Raman scattering at the silver electrode/ionic liquid (BMIPF₆) interface. *J. Phys. Chem. B* **2006**, *110* (41), 20379-20385.
- 154. García Rey, N.; Dlott, D. D., Structural transition in an ionic liquid controls CO₂ electrochemical reduction. *J. Phys. Chem. C* **2015**, *119* (36), 20892-20899.

- 155. Kemna, A.; Braunschweig, B., Potential-induced adsorption and structuring of water at the Pt(111) electrode surface in contact with an ionic liquid. *J. Phys. Chem. Lett.* **2020**, *11* (17), 7116-7121.
- 156. Liu, S.; Peng, J.; Chen, L.; Sebastian, P.; Feliu, J. M.; Yan, J. W.; Mao, B. W., In-situ STM and AFM studies on electrochemical interfaces in imidazolium-based ionic liquids. *Electrochim. Acta* **2019**, *309*, 11-17.
- 157. Gnahm, M.; Pajkossy, T.; Kolb, D. M., The interface between Au(111) and an ionic liquid. *Electrochim. Acta* **2010**, *55* (21), 6212-6217.
- 158. Li, H.; Endres, F.; Atkin, R., Effect of alkyl chain length and anion species on the interfacial nanostructure of ionic liquids at the Au(111)–ionic liquid interface as a function of potential. *Phys. Chem. Chem. Phys.* **2013**, *15* (35), 14624-14633.
- 159. Cui, T.; Lahiri, A.; Carstens, T.; Borisenko, N.; Pulletikurthi, G.; Kuhl, C.; Endres, F., Influence of water on the electrified ionic liquid/solid interface: A direct observation of the transition from a multilayered structure to a double-layer structure. *J. Phys. Chem. C* **2016**, *120* (17), 9341-9349.
- 160. Ramirez-Cano, J. A.; Veleva, L., Direct measurement of the adsorption kinetics of 2-Mercaptobenzothiazole on a microcrystalline copper surface. *Revista De Metalurgia* **2016**, *52* (1).
- 161. Medina-Ramos, J.; Lee, S. S.; Fister, T. T.; Hubaud, A. A.; Sacci, R. L.; Mullins, D. R.; DiMeglio, J. L.; Pupillo, R. C.; Velardo, S. M.; Lutterman, D. A.; Rosenthal, J.; Fenter, P.,

Structural dynamics and evolution of bismuth electrodes during electrochemical reduction of CO₂ in imidazolium-based ionic liquid solutions. *ACS Catal.* **2017**, *7* (10), 7285-7295.